Nanoscale Advances

ROYAL SOCIETY OF CHEMISTRY

REVIEW

View Article Online
View Journal | View Issue

Cite this: *Nanoscale Adv.*, 2024, **6**, 318

Multicomponent chiral plasmonic hybrid nanomaterials: recent advances in synthesis and applications

Guizeng Yang, Lichao Sun* and Qingfeng Zhang *

Chiral hybrid nanomaterials with multiple components provide a highly promising approach for the integration of desired chirality with other functionalities into one single nanoscale entity. However, precise control over multicomponent chiral plasmonic hybrid nanomaterials to enable their application in diverse and complex scenarios remains a significant challenge. In this review, our focus lies on the recent advances in the preparation and application of multicomponent chiral plasmonic hybrid nanomaterials, with an emphasis on synthetic strategies and emerging applications. We first systematically elucidate preparation methods for multicomponent chiral plasmonic hybrid nanomaterials encompassing the following approaches: physical deposition approach, galvanic replacement reaction, chiral molecule-mediated, chiral heterostructure, circularly polarized light-mediated, magnetically induced, and chiral assembly. Furthermore, we highlight emerging applications of multicomponent chiral plasmonic hybrid nanomaterials in chirality sensing, enantioselective catalysis, and biomedicine. Finally, we provide an outlook on the challenges and opportunities in the field of multicomponent chiral plasmonic hybrid nanomaterials. In-depth investigations of these multicomponent chiral hybrid nanomaterials will pave the way for the rational design of chiral hybrid nanostructures with desirable functionalities for emerging technological applications.

Received 22nd September 2023
Accepted 30th November 2023

DOI: 10.1039/d3na00808h

rsc.li/nanoscale-advances

1. Introduction

Chirality permeates various scales within biological systems, spanning from the molecular to the macroscopic level.[1] The unique influence of chirality on the structure and function of biomolecules arises from their non-superimposable geometric configurations. Following the pioneering work of Louis Pasteur in 1848,[2] wherein he reported on the optical rotation properties of distinct tartaric acid crystals, the concept of chirality has undergone an expansion beyond molecular configurations, encompassing a broad range of compounds, including amino acids, proteins, and diverse inorganic entities.[3–5] In recent years, the remarkable attributes of chiral inorganic materials have

College of Chemistry and Molecular Sciences, Wuhan University, Wuhan 430072, China. E-mail: lichaosun@whu.edu.cn; zhangqf@whu.edu.cn

Guizeng Yang

Guizeng Yang received his BS degree in chemistry from Shenyang Agricultural University in 2018 and his MS degree in physical chemistry from Fuzhou University in 2021, respectively. He is currently a PhD candidate working on chiral plasmonic nanomaterials under the supervision of Qingfeng Zhang at the Wuhan University.

Lichao Sun

Lichao Sun completed her BS in chemistry at the Dalian University of Technology in 2009. She received her MS in inorganic chemistry from Xiamen University in 2012, and her PhD in chemistry from the University of South Carolina, USA. She is currently a lecturer in the College of Chemistry and Molecular Sciences at Wuhan University. Her research interests include functional inorganic nanomaterials and their applications in chirality and catalysis.

propelled the burgeoning interest in chiral materials.[3,6–9] In particular, structurally chiral plasmonic nanomaterials show significantly larger scattering and absorption cross-sections and chiroptical activities than other chiral inorganic materials owing to their inherent plasmonic properties.[10–12] Thus, this review article primarily focuses on elucidating the characteristics and applications of chiral plasmonic materials.

Noble metals such as Au and Ag exhibit intriguing plasmonic properties due to their strong light–matter interactions.[13,14] For metal nanoparticles (NPs), the collective oscillations of free electrons are confined by the particle boundaries over nanoscale geometric dimensions upon light excitation phenomenon, known as localized surface plasmon resonance (LSPR).[15] Resonant phenomena occur when the frequency of light matches the intrinsic frequency of the collective oscillations of electrons in metal NPs (Fig. 1a). The resonance peak position and intensity of LSPR strongly depend on the size, shape, composition, and refractive index of the surrounding medium of the metal NPs. Therefore, precise tailoring of the NP morphology enables the realization of plasmonic NPs with tunable plasmonic properties such as Au nanorods (NRs),[16] nanoshells,[17–19] and nanocages.[20–22] Furthermore, the collective oscillation of free electrons in metal nanoparticles (NPs) under resonant excitation gives rise to a range of intriguing phenomena. These include enhanced light absorption or scattering at resonance frequencies, a significant amplification of the electromagnetic field intensity on the surface of the nanoparticles, localized photothermal generation, and the generation of transient high-energy hot electrons and holes that deviate from thermal equilibrium.[18,23,24] As shown in Fig. 1b, numerical simulations such as Mie theory or finite-difference time-domain reveal that closely spaced Au NP dimers exhibit much stronger electromagnetic field enhancement compared to individual Au NPs.[19] The localized and highly intense electromagnetic fields, created in junctions between adjacent NPs, are often referred to as plasmonic hot spots. Further coupling the intense plasmonic near-fields with surface-adsorbed molecules creates vast opportunities for the application of plasmonic nanomaterials in various fields, including sensing,[25–28] catalysis,[23,28,29] and surface-enhanced Raman spectroscopy (SERS).[30,31] For a more comprehensive understanding of the plasmon, we recommend that readers read some review articles that have been published on this topic.[13,15,32,33] To summarize, due to the intense and tunable optical properties of metal NPs, the integration of plasmonic characteristics with chirality provides a promising approach to construct chiral plasmonic NPs with an intrinsic chiral structure and geometry-dependent optical chirality.

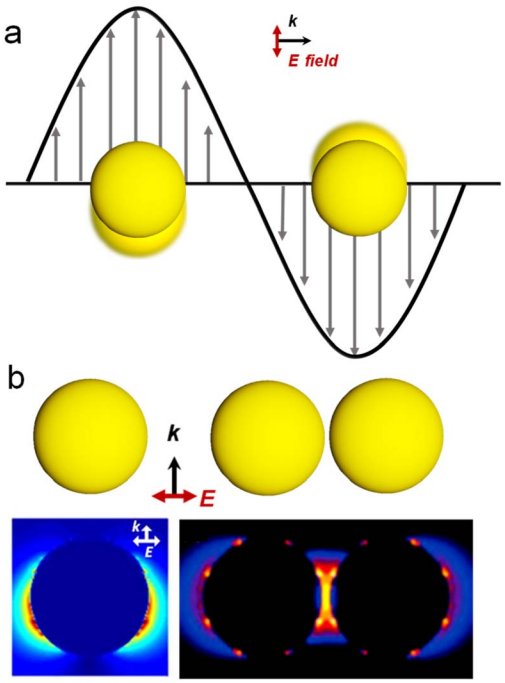

Fig. 1 Optical properties of plasmonic NPs. (a) Localized surface plasmon resonance of Au NPs. (b) Calculated distribution of electromagnetic near-field enhancements of a single Au NP and Au NP dimer.[14] Reproduced from ref. 14 with permission from American Chemical Society, copyright 2005.

Chirality can be manifested not only in the inability of chiral structures to overlay with their mirror images but also in the optical phenomenon known as circular dichroism (CD), where optically active chiral structures exhibit differential absorption of left-handed circularly polarized (LCP) and right-handed circularly polarized (RCP) light.[27,34,35] Unlike the mismatch in size and wavelength between chiral molecules and light, plasmonic nanomaterials possess distinct field enhancement and plasmon resonance. Therefore, when interacting with light, plasmonic nanomaterials not only enhance the chiral response of molecules but also induce excited plasmonic modes that can span the entire chiral nanoparticle, resulting in pronounced optical responses. For the chiral assembly of plasmonic NPs, the plasmon–plasmon coupling among the chiral-arranged plasmonic nanoparticles created the differential extinction over the LCP/RCP light, whereas the individual plasmonic nanoparticles are achiral. Different from the mechanism of chiral assembly, chirality can also originate from the plasmonic NPs with intrinsic chiral structures. In this case, the chiral

Qingfeng Zhang

Qingfeng Zhang is a professor in the College of Chemistry and Molecular Sciences at Wuhan University, China. He received his PhD from the University of South Carolina in 2017. He then worked as a J. Evans Attwell-Welch Postdoctoral Fellow at Rice University, USA. He joined Wuhan University as a full professor in 2020. His research interests encompass the development of novel nanoscale spectroscopic imaging tools to quantify heterogeneities, kinetics, and thermodynamics of single particles in next-generation functional materials, particularly in the areas of plasmonics, chirality, and catalysis.

plasmonic NPs also interact differently with LCP/RCP light due to the intrinsic chiral plasmons. Both mechanisms have been presented in Fig. 2 with detailed discussions.

Plasmon-coupled CD is a typical example where plasmonic nanomaterials exhibit interesting chiroptical activity when they undergo strong interactions with chiral molecules. Govorov and co-workers have shown that chiral molecules in proximity to achiral plasmonic NPs can induce CD at the NP's LSPR due to coulombic (dipole and multipole) interactions between the chiral molecule and achiral plasmonic object. The near-fields of achiral plasmonic NPs can increase the strength of the CD signal at the molecular absorption frequency, and also intriguingly, the CD signal also occurs at the plasmon resonance.[25] Unlike the mismatch in size and wavelength between chiral molecules and light, plasmonic nanomaterials possess distinct field enhancement and plasmon resonance. Therefore, when interacting with light, plasmonic nanomaterials not only enhance the chiral response of molecules but also induce excited plasmonic modes that can span the entire chiral nanoparticle, resulting in pronounced optical responses. Gansel and co-workers reported a square array composed of independent 3D gold helices fabricated by combining direct laser writing and electrochemical deposition. The array performs a high transmittance difference between LCP/RCP in a broadband spectral range, which enables it an excellent circular polarizer.[36] Due to the diversity of interactions between chiral plasmonic nanomaterials and substances from the distinct surface ligands and chiral crystal facets. This makes plasmonic nanomaterials highly promising for applications in asymmetric catalysis,[37,38] enantioselective sensing,[39–41] biomedicine,[42,43] *etc.*

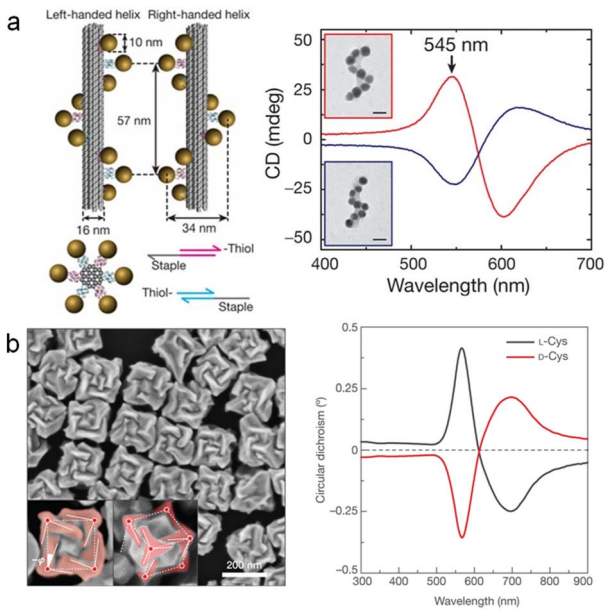

Fig. 2 Typical structures of chiral plasmonic nanomaterials. (a) Chiral assembly of Au NPs templated by DNA origami.[44] Reproduced from ref. 44 with permission from Springer Nature, copyright 2012. (b) Chiral Au NPs with an intrinsic chiral structure prepared by the seed-mediated chiral growth method.[50] Reproduced from ref. 50 with permission from Springer Nature, copyright 2018.

Thus, plasmonic chirality has garnered significant interest over the past decade. Based on the design of chiral plasmonic nanostructures, two typical structures of plasmonic nanostructures with intrinsic chiral structures have been demonstrated. The first structure is the chiral assembly of plasmonic NPs to mimic the helical structure of biomolecules, such as DNA. In particular, Liedl and co-workers employed DNA origami techniques to precisely control the helical arrangement of Au NPs (Fig. 2a).[44] They hybridized short oligonucleotide chains onto long single-stranded DNA scaffolds, forming one-dimensional helical structures that enabled self-assembly of Au NPs with complementary strands into nanoscale helical structures. The assembled helical Au NPs exhibited strong CD responses in the visible spectral region due to the plasmonic properties of Au NPs. The plasmon–plasmon coupling among the chiral arranged Au NPs created the differential extinction over the LCP/RCP light. Furthermore, in the context of DNA-mediated chiral structure design, control over polarized light from visible to near-infrared wavelengths was achieved by manipulating structures such as Au NRs dimers,[45] tetramers,[46] and nanorings.[47]

Another approach to constructing chiral plasmonic structures involves the design of discrete plasmonic NPs with inherent geometric chirality, especially with the rapid development of wet-chemical synthesis methods in recent years, greatly expanding the family of chiral plasmonic materials.[48,49] As shown in Fig. 2b, Nam and co-workers employed small chiral molecules (amino acids and peptides) as chiral inducers to guide the growth of surfaces with high Miller indices {321} facets, forming twist sites and breaking crystal symmetry through the 432-point group symmetry to grow into chiral structures.[50] Experimental results demonstrated that chiral molecules of cysteine (Cys) L-Cys and D-Cys could induce the growth of Au nanocubes, resulting in perfect mirror symmetry and superior chiroptical responses. Additionally, when the chiral molecules were further extended to glutathione (GSH), each surface of the chiral NPs formed unique highly curved gaps, leading to a strong asymmetric factor of the chiral NPs (asymmetric factor of 0.2). These results indicate that the interaction between chiral molecules and the crystal plane is a crucial factor in the transfer of chirality from chiral molecules to plasmonic materials. It is evident that wet chemical methods offer a promising strategy for the realization of discrete chiral nanostructures at various hierarchical levels. This approach has significantly expanded the compositional diversity of chiral nanomaterials, enabling the fabrication of a wide range of chiral plasmonic NPs. Notably, there are also other types of chiral plasmonic structures, such as planar chiral plasmonic structures with superchiral near-fields, which exhibit intriguing sensing capability over chiral molecules.[51–54]

For a more comprehensive overview of chiral plasmonic nanomaterials, we encourage readers to read some recently published reviews for more details.[10,55–58] Compared to chiral nanomaterials with monocomponent, chiral structures with multiple components provide a promising approach to the integration of desired chirality with other functionalities into one single nanoscale entity. The synergistic couplings among different components could potentially create interesting

properties and have inspired promising applications. On the other hand, there have been numerous excellent reviews on single-component chiral plasmonic nanomaterials, however, very limited reviews specifically dedicated to multicomponent chiral hybrid plasmonic nanomaterials are available. Given the rapid advancement of this field, we believe it is timely and crucial to provide a systematic overview of this field. Therefore, our focus is primarily on multicomponent chiral plasmonic hybrid nanomaterials.

Over the past decade, there has been in-depth research on the structure,[50,59,60] optical activity,[27,36,61–64] and theoretical calculations of chirality,[35,65,66] leading to successful applications in catalysis, sensing, and biomedicine. Despite significant efforts in the preparation and application of chiral plasmonic nanomaterials, substantial challenges remain when confronted with more complex application scenarios. The "multicomponent nanomaterials" can be defined as hybrid structures composed of two or more distinct and definable condensed nanodomains, which differ in material composition, shape, or size. Introducing new components into single-component chiral plasmonic nanomaterials to construct multicomponent chiral plasmonic hybrid nanomaterials provides a broad avenue for exploration. The synergistic couplings among different components could potentially create interesting properties and have inspired promising applications in asymmetric catalysis, photonics, and so forth.[67–69] For instance, chiral TiO_2-Au heterostructures were constructed as plasmon-based photocatalysts with polarization-dependent reactivity.[67] Selectively coupling the magnetic component with the semiconductor structure can generate chiral optical activity mediated by magnetic fields.[70] Despite these pioneering efforts, the construction of desired functional components onto chiral plasmonic structures in a controllable manner remains largely unexplored. Therefore, we believe it is timely to circumnavigate the preparation and emerging applications of multicomponent chiral plasmonic hybrid nanomaterials and widen the scope of their potential applications.

In this review, we present the recent advances in the synthesis, properties, and application of multicomponent chiral plasmonic hybrid nanomaterials (Fig. 3). We first discuss the preparation of multicomponent chiral plasmonic hybrid nanomaterials through several physical and chemical approaches, including physical deposition method, chiral molecule-mediated growth method, chiral heterostructure, CPL-mediated, magnetically induced, and chiral assembly. Additionally, we highlight three emerging application prospects of multicomponent plasmonic hybrid nanomaterials including sensing, catalysis, and biomedicine. Finally, we provide an outlook on the challenges and opportunities for the field of multicomponent chiral plasmonic hybrid nanomaterials.

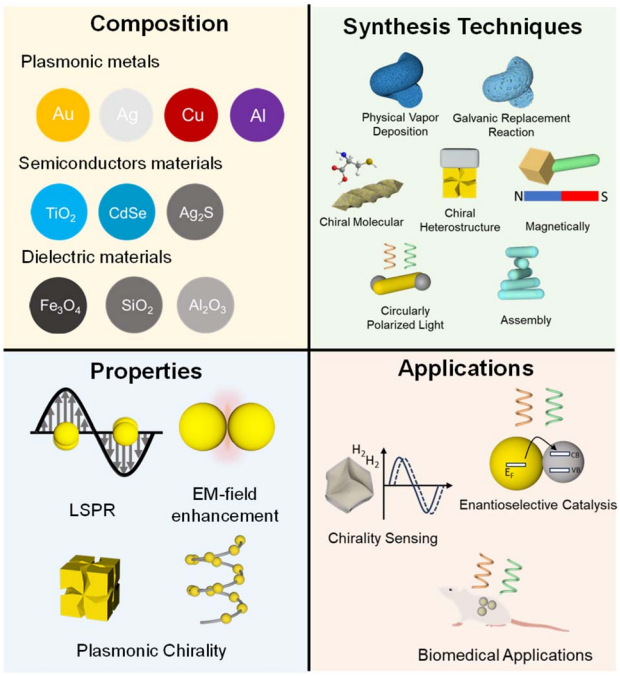

Fig. 3 Overview of the preparation, properties, and emerging applications of multicomponent chiral plasmonic hybrid nanomaterials.

2. Synthesis of multicomponent chiral plasmonic hybrid nanomaterials

Over the past two decades, the preparation methods for chiral nanomaterials have gradually matured, leading to a deepening understanding and extensive research on the chiral effects. Especially with regards to current chiral plasmonic materials, due to their advantages in controllable synthesis through wet chemical methods, they are mostly limited to Au, rather than other metals such as Pt, Pd, and Cu, which exhibit higher catalytic activity in many important catalytical reactions. Therefore, the integration of multiple components into chiral plasmonic nanomaterials has endowed them with potential new functionalities, greatly expanding the catalytic prospects of chiral plasmonic nanomaterials. In this section, we first discussed the methods of fabricating intrinsic chiral multicomponent materials through a one-step process, including Section 2.1 chiral molecule-induced and Section 2.2 physical deposition approaches. Secondly, we present the methods that create multicomponent chiral structures using chiral monocomponent as templates, including Section 2.3 galvanic replacement reactions and Section 2.4 chiral heterostructure. Finally, we discuss the methods of inducing and assembling multicomponent chiral plasmonic nanomaterials using external stimulus, including Section 2.5 circularly polarized light-mediated growth, Section 2.6 magnetically induced chirality, and Section 2.7 chiral assembly.

2.1 Chiral molecule-mediated growth

The precise manipulation of multicomponent chiral hybrid nanomaterials fabrication is of paramount significance in expanding the multifunctional applications of chiral nanomaterials. However, the preparation of multicomponent chiral plasmonic hybrid nanomaterials still represents a significantly challenging task. Recent advancements in the development of efficient techniques for fabricating chiral materials have offered

novel prospects for creating multicomponent chiral plasmonic materials with desired geometric chirality and functionality. The wet-chemical synthesis method provides a promising strategy for fine-controlling the geometry of multicomponent chiral plasmonic hybrid NPs with increasing architectural complexity and compositional diversity. The introduction of chiral molecules in the wet chemical synthesis process offers a simple and effective approach for generating chiral plasmonic nanomaterials with remarkable optical activity.[50,71–73] The specific interactions between chiral molecules and crystal facets play a crucial role in inducing chiral growth.[74] One way to create chiral hybrid materials is to build on the seed-mediated chiral growth method. Wu and co-workers developed a strategy for the synthesis of AuAg helical NRs through the cooperative induction of dual thiols (Fig. 4a).[75] Chiral AuAg NRs were formed by co-reduction of Au and Ag atoms on Au NRs modified by Cys and 4-aminothiophenol molecules. Furthermore, this method allowed for the tuning of the chiral optical activity by controlling parameters such as the aspect ratio of Au NRs, the Au/Ag atomic ratio, and the concentration of thiol, with a maximum anisotropy factor reaching 0.04. An alternative strategy to prepare chiral alloy NRs was developed by Liz-Marzán and co-workers, which built on the use of chiral cosurfactants as templates for the seed-mediated chiral growth of Au NR.[76–78] They employed chiral micelles formed by chiral ligands (BINOL, 1,1′-bi(2-naphthol)) and hexadecyl trimethyl ammonium chloride (CTAC) as templates to achieve the co-reduction of Au and Pd/Pt atoms on Au NRs, resulting in the formation of chiral AuPd and AuPt alloy NRs with tunable composition and optical chirality (Fig. 4b).[76–78]

Interestingly, the chirality transfer from chiral molecules to multicomponent alloy materials can be also achieved in a substrate-induced growth procedure, which is significantly different from that in colloidal solutions with a seed-mediated chiral growth process.[41] Particularly, Che and co-workers employed *N*-acetyl-L/D-cysteine (S/R-NAC) as a chiral inducer on Si substrates, with $HAuCl_4$ and $AgNO_3$ as precursors, to electrochemically generate chiral AuAg bimetallic films (Fig. 4c).[79] SEM and TEM images revealed that the films grew perpendicular to the substrate, forming polycrystalline Boerdijk–Coxeter–Bernal (BCB) four-fold helical structures composed of AuAg alloy. CD diffuse reflectance spectra indicated chiroptical signals at 545 nm for the entire substrate, exhibiting mirror-image symmetry influenced by the chirality of the molecules. It was further demonstrated that the chiral AuAg alloy nanowires (NWs) could serve as a chiral platform for enantiomer recognition. Moreover, the chiral molecule-mediated growth method can be also extended to create chiral metal–semiconductor hybrid structures. For example, Wang and co-workers employed Au octahedra as seeds and cysteine–phenylalanine (Cys–Phe) as a chiral agent to induce the selective growth of PbS at the vertices of the Au octahedra, resulting in pronounced chiral optical activity.[80] To summarize, the chiral molecule-mediated growth method is a versatile and robust strategy to achieve multicomponent chiral nanomaterials with controllable shape and composition, offering potential platforms for investigations of geometry-dependent chiroptical properties of the chiral hybrid materials.

2.2 Physical deposition approaches

The physical methods for fabricating chiral materials are considered promising strategies. Currently, several physical techniques such as focused electron beam-induced deposition

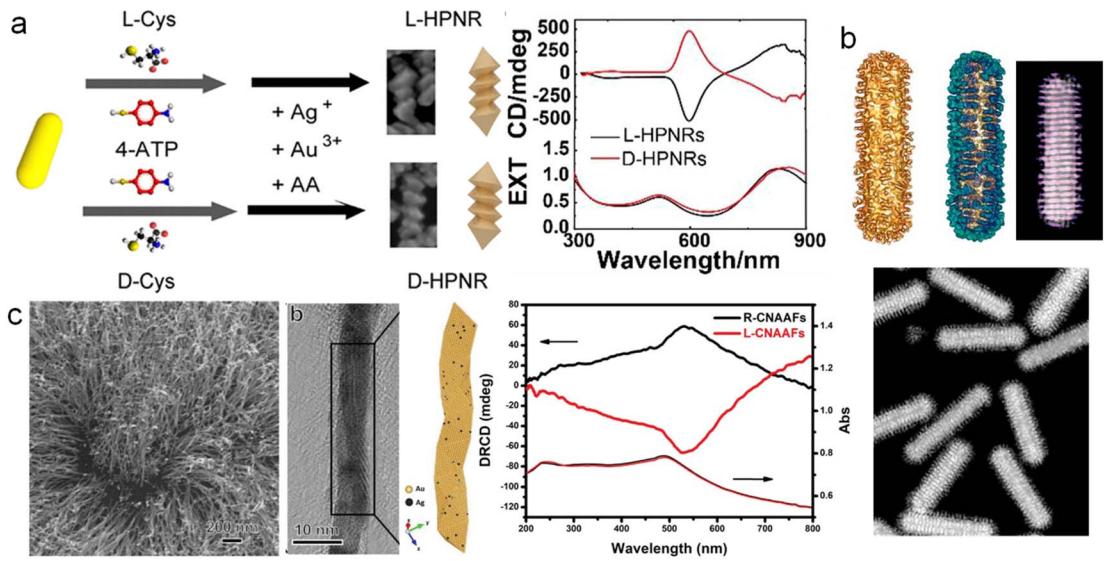

Fig. 4 Multicomponent chiral plasmonic hybrid nanostructures prepared by the chiral molecule-mediated growth method. (a) Chiral AuAg alloy NRs prepared through the seed-mediated co-deposition of Au and Ag in the presence of L/D-Cys.[75] Reproduced from ref. 75 with permission from American Chemical Society, copyright 2021. (b) Chiral Au–Pt NRs with quasihelical surface patterns generated by the templating effect of chiral bi-surfactant micelles.[77] Reproduced from ref. 77 with permission from AAAS, copyright 2020. (c) Chiral AuAg NWs prepared by electrochemical reduction processes in the presence of *N*-acetyl-L/D-Cys.[79] Reproduced from ref. 79 with permission from Wiley VCH, copyright 2022.

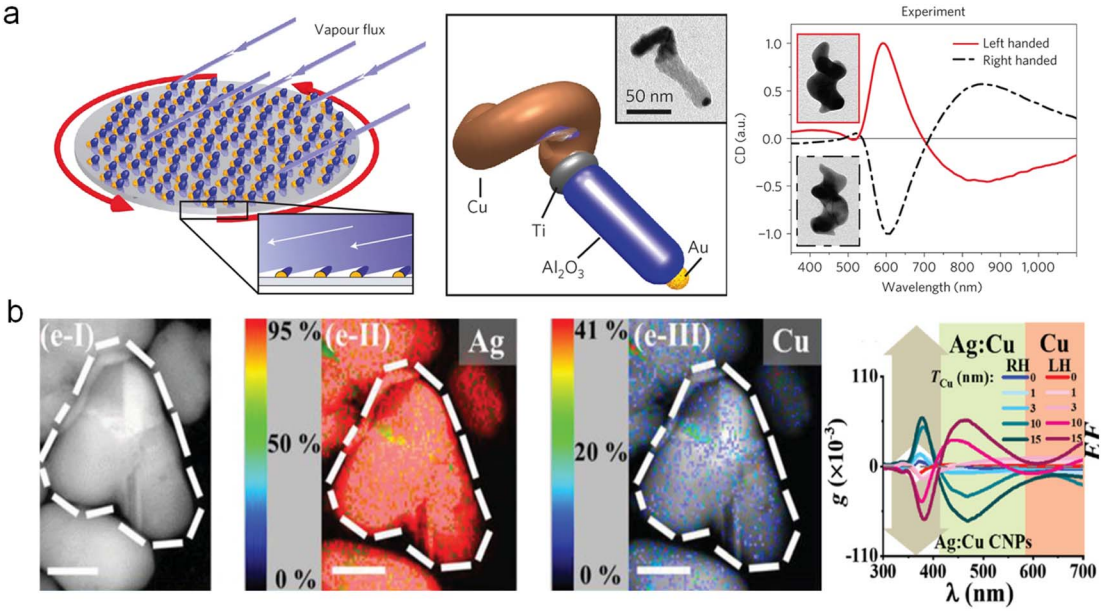

Fig. 5 Multicomponent chiral hybrid nanomaterials prepared by the physical deposition method. (a) Chiral hybrid nanocolloid through low-temperature shadow deposition.[84] Reproduced from ref. 84 with permission from Springer Nature, copyright 2013. (b) AgCu chiral NPs created through the glancing angle co-deposition method.[87] Reproduced from ref. 87 with permission from Wiley VCH, copyright 2020.

(FEBID),[81] photolithography,[82] and stepwise glancing angle deposition[83] have been employed to construct chiral structures with single components in multiple dimensions. These methods provide new insights into the fabrication of multicomponent chiral hybrid nanomaterials. For example, Fischer and co-workers have further overcome the inherent symmetry constraints in the growth of small structures by utilizing a physical vapor deposition technique to fabricate multicomponent chiral hybrid nanomaterials. These structures exhibit CD optical activity and allow for high-throughput manufacturing (Fig. 5a).[84]

Furthermore, physical vapor deposition also enables the fabrication of chiral alloy NPs with controllable composition and optical chirality. Huang and co-workers have demonstrated a physical fabrication approach for creating chiral alloy NPs (Fig. 5b).[85,86] By leveraging physical vapor deposition, they devised the glancing angle deposition (GLAD) technique, which entails controlling substrate rotation to achieve rapid substrate rotation-driven manipulation of deposition angles, facilitating the production of monometallic chiral NPs such as Ag, Cu, and Al with remarkable optical chirality. They further advanced the field by employing a three-step consecutive GLAD method for the synthesis of multi-metal chiral alloy NPs. In a typical procedure, they utilized single-component chiral NPs as the initial material, and solute M (Cu, Fe, Al) atoms were thermally driven to diffuse into the substrate and align in a chiral manner. This process enabled the replication of the substrate's chirality and led to the formation of chiral alloy NPs.[87] Experimental findings substantiated that this approach not only enabled the fabrication of multicomponent chiral hybrid nanomaterials but also amplified the plasmonic optical activity of the resulting chiral NPs, thus establishing a robust foundation for the development of versatile chiral platform.

2.3 Galvanic replacement reaction

Not only can multicomponent chiral hybrid nanomaterials with intrinsic chirality be achieved through molecular-induced and physical deposition methods, but it is also possible to create multicomponent chiral plasmonic hybrid nanomaterials by introducing new components onto a single-component chiral nanomaterial. Galvanic Replacement Reaction (GRR) is an effective chemical method that utilizes the difference in electrochemical reduction potential between the sacrificial template and the returning material to achieve porous nanostructures.[82,83] Currently, a variety of shaped and compositional nanomaterials have been successfully fabricated using the GRR method. One example is Qin and coworkers synthesized concave AuAg alloy frame Ag nanocubes through a dropwise addition of $HAuCl_4$ (Fig. 6a).[88] This method allows for selective substitution and deposition at different positions by controlling the NaOH in the reaction. Furthermore, interesting variations in chirality templates occur when sacrificial templates possess chiral structures. In particular, Huang and co-workers combined the GLAD with GRR to achieve the chirality transfer from monocomponent to multicomponent chiral structures.[89] They employed the sacrificial template strategy within the context of GRR by employing sacrificial Ag chiral NPs prepared *via* the GLAD method (Fig. 6b).[89] The sacrificial templates were subjected to GRR within a solution containing ions possessing higher electrode potentials, such as Au^{3+}. After the GRR, the chiral AgAu alloy NPs showed a porous structure, and the CD spectrum showed obvious redshift and broadening. Remarkably, the GRR phenomenon facilitated the formation of porous multicomponent chiral alloy nanomaterials, including CuAg, AgAu, AgPt, and AgPd, thereby enabling the transfer of chirality from single-component NPs to multicomponent NPs.

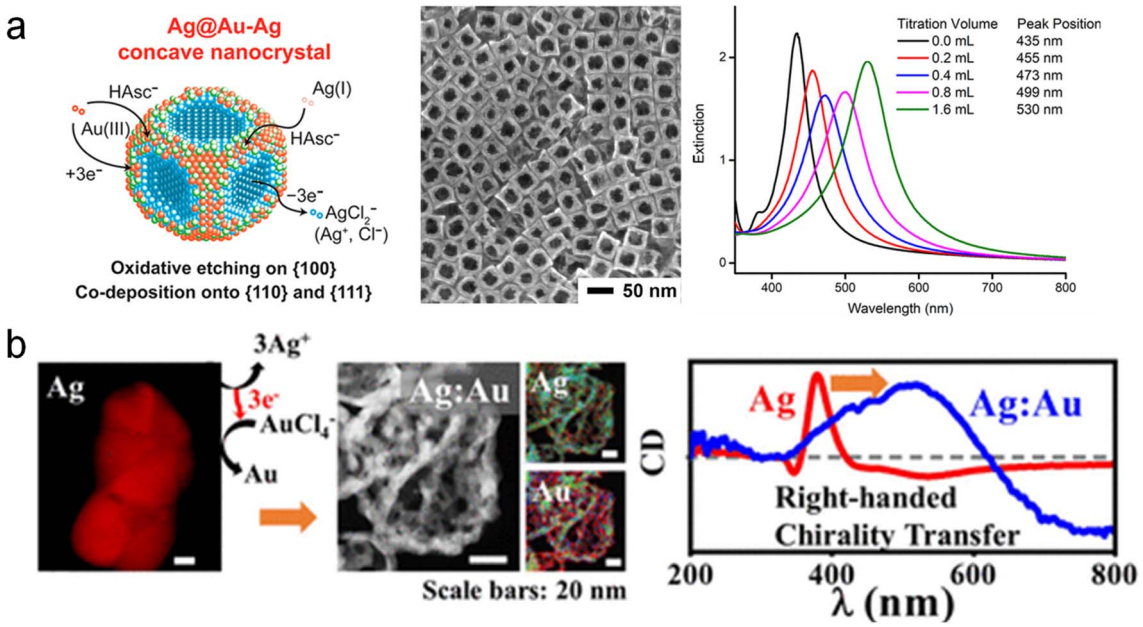

Fig. 6 Multicomponent chiral hybrid nanomaterials prepared by galvanic replacement reactions. (a) AuAg alloy NPs prepared by site-selective GRR between Au ion and Ag NPs.[88] Reproduced from ref. 88 with permission from American Chemical Society, copyright 2018. (b) AuAg chiral alloy NPs prepared by GRR of Au ion and Ag chiral NPs.[89] Reproduced from ref. 89 with permission from American Chemical Society, copyright 2019.

Furthermore, by extending the sacrificial template approach to the CuAu system encompassing two components,[90] the inert Au component served as a scaffold, supporting the chiral transfer of the third metal (Pt/Ag) and ultimately giving rise to the formation of ternary chiral NPs. On the other hand, cation exchange is another effective method for constructing multicomponent materials and holds promise for the fabrication of multicomponent chiral hybrid materials.[91] In summary, the GRR is a powerful method for the fabrication of chiral alloy structures with porous features. It is envisioned that the as-prepared porous chiral alloy NPs could potentially serve as excellent catalysts for enantioselective molecular reactions.

2.4 Chiral heterostructure

The construction of heterogeneous structures is a promising method for preparing multicomponent chiral hybrid nanomaterials. Core–shell structures and Janus structures can be formed in various groups due to the influence of the surface energy of different components. The diverse activities brought by such heterogeneous structural differences make it widely used in nanoelectronics, catalysis, and biomedicine.[92–94] So far, the formation of chiral materials has been limited to Au, Ag, and some other inorganic materials. Thus, using the chiral NPs as templates to overgrow achiral materials represents a promising way to create multicomponent chiral hybrid materials with increasing compositional diversity. For example, Nam and co-workers deposited a cobalt (Co) thin film onto uniformly aligned chiral Au helicoids, achieving controllable magnetic CD optical activity by tuning the spacing and dimensions of the chiral Au helicoids (Fig. 7a).[95] By manipulating the magnetic field, the chiral Au helicoid exhibited tunable CD values ranging from 0.9° to 1.5° at a wavelength of 550 nm. The integration of chiral plasmonic materials with magnetic components allows the realization of using the magnetic field to control the optical chirality, which has promising applications in nanophotonics, optical displays, and optical switches.

Seed-mediated growth method using chiral NPs as seeds provides a versatile strategy for constructing chiral plasmonic heterostructures. It has been demonstrated that chiral Au NPs can serve as seeds for the overgrowth of achiral metal, silica, and semiconductor components. As depicted in Fig. 7b, chiral Au NRs were used as seeds for the growth of SiO_2 in a solution of (3-mercaptopropyl)trimethoxysilane (MPTMS). After encapsulation with SiO_2, the extinction and CD spectra of the chiral Au NRs exhibited a slight redshift.[96] Theoretical calculations indicated that this shift was caused by changes in the dielectric constant induced by SiO_2. Similarly, for the preservation of chiral NPs, SiO_2, polyisobutylene-alt-maleic anhydride (PMA), and polydopamine (PDA) were used as protective coatings on chiral nanoparticles, with all three providing protection, with PDA demonstrating the best performance.[76] Moreover, Nam and co-workers also achieved capacitively coupled strong electric and magnetic resonances by growing SiO_2 to construct chiral metal-insulator-metal (MIM) resonators.[97] Interestingly, Ouyang and co-workers performed semiconductor modifications on chiral Au NPs. They initially grew Ag on chiral Au NPs and subsequently converted them to Au@Ag_2S and Au@CdS core–shell NPs through multiple-step transformations. These structures exhibited intriguing structure-dependent optical chirality.[69] Considering the interaction between plasmons and semiconductors, such structures hold promise in chiral photocatalysis.

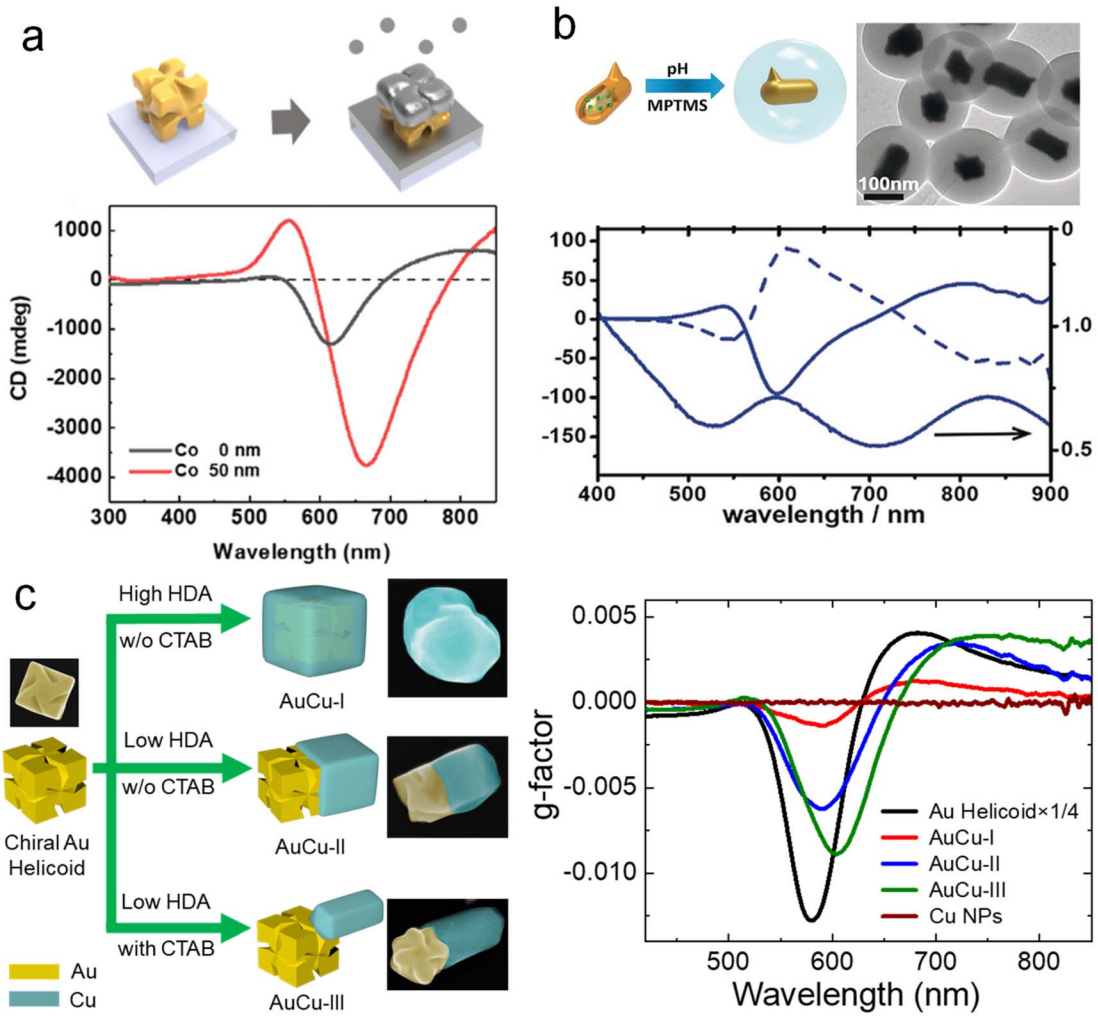

Fig. 7 Chiral plasmonic heterostructures. (a) Schematic diagram of heterostructures produced by Co deposition of chiral Au helicoid and the CD spectra.[95] Reproduced from ref. 95 with permission from American Chemical Society, copyright 2022. (b) Chiral Au-SiO_2 heterostructures generated by overgrowth chiral Au NRs with silica and the corresponding CD and extinction spectra.[96] Reproduced from ref. 96 with permission from Wiley VCH, copyright 2018. (c) Site-specific growth of chiral Au–Cu heterostructures and the corresponding CD spectra.[98] Reproduced from ref. 98 with permission from Springer Nature, copyright 2023.

More recently, Zhang and co-workers demonstrated the site-specific geometric control of chiral AuCu heterostructures with diverse architectures and tailored optical chirality (Fig. 7c).[98] By simply manipulating the concentrations of the surfactants hexadecylamine (HDA) and cetyltrimethylammonium bromide (CTAB), they achieved the selective deposition of Cu nanodomains on chiral Au NPs. Chiral AuCu heterostructures with three distinct architectures were achieved by controlling the overgrowth of Cu nanodomains in a site-specific manner. They further experimentally and theoretically demonstrated the correlation between the optical and CD properties of chiral AuCu heterostructures and their distinct geometric feature. This method can be extended to different chiral Au NPs, including isotropic and anisotropic 3D, 2D, and 1D chiral Au NPs. Despite these pioneering efforts, constructing desired functional components in a controllable manner on chiral plasmonic structures remain a significant challenge. Additionally, the understanding of the plasmonic coupling between chiral plasmonic structures and achiral or non-plasmonic components remains largely unexplored. Therefore, further efforts are required for the rational design of multifunctional chiral plasmonic hybrid materials to expand their applications in various emerging technological fields.

2.5 Circularly polarized light-mediated growth

The strong interaction between plasmon and resonant photons enables its utilization as a nanoscale antenna to employ light to drive chemical transformations on surfaces of plasmonic NPs.[99–101] Thus, it is envisioned that using circularly polarized light (CPL) to create chiral hybrid plasmonic materials provides a promising avenue for the chirality transfer from CPL to materials.[102] For example, Kotov and co-workers demonstrated the formation of Au NPs by illuminating Au^{3+} precursor solution with CPL, which subsequently assembled into chiral nanostructures with diameters of 10–15 nm.[103] Moreover, Xu and co-

workers reported seed-mediated growth processes under CPL irradiation, resulting in the formation of chiral Au NPs with an asymmetric factor of 0.4.[42] However, the above results are mostly limited to single component chiral plasmonic materials, the fabrication of multicomponent chiral hybrid plasmonic nanomaterials mediated by CPL are significantly more challenging.

An intriguing strategy is the utilization of plasmonic hot carriers excited by CPL for the chiral growth of other plasmonic or non-plasmonic components onto the plasmonic substrates. Particularly, Tatsuma and co-workers fabricated chiral plasmonic hybrid structures through selective LH/RH CPL irradiation, which induces the asymmetric distribution of plasmonic hot carriers (Fig. 8a).[104,105] Achiral Au NRs were selected as seeds and placed on a TiO_2 substrate to facilitate charge separation. CPL was then irradiated to localize the electric field to specific corners of the NRs, generating high-energy holes at localized sites for the reduction of Pb precursors and allowing the deposition of PbO_2 at specific corners. Under LH/RH CPL irradiation, mirror-symmetric chiral structures and CD spectra were observed.

Moreover, Govorov and co-workers conducted in-depth investigations of this strategy and proposed a theoretical approach involving high-energy hot electrons locally mediated by light excitation for the non-uniform growth of nanostructures (Fig. 8b). The results simulated by this theoretical model are in good agreement with Tatsuma's results.[65] Additionally, through the simulations of different geometric models under CPL irradiation, it was demonstrated that the injection rate of localized hot carriers is a key factor in inducing non-uniform deformation in Au NPs. This theoretical model provides new insights for a profound understanding of CPL-mediated growth of chiral plasmonic materials. Moreover, Xu, Kotov, and co-workers demonstrated that the combination of CPL irradiation with chiral additives leads to geometrically controllable chiral Au NPs with significantly enhanced optical anisotropy factors (*g*-factors) of up to 0.44 (Fig. 8c).[42] The integration of CPL-mediated growth with chiral molecule-induced strategies in the synthetic procedure could be further expanded to apply in the formation of chiral multicomponent hybrid materials.

2.6 Magnetically induced chirality

As is well-known, chirality and magnetic fields are closely intertwined. Therefore, various chiral assemblies have been realized by the induction of magnetic fields.[106] However, magneto-induced chirality of discrete NPs is rarely reported. Weak magnetic moments play a significant role in limiting the coupling between the magnetic field of photons and the magnetic moments of electrons during light–matter interactions. Therefore, the preparation of nanomaterials that combine strong magnetic optical properties with chirality is of great importance. An intriguing strategy to achieve magnetically induced chirality in achiral materials is the regioselective magnetization of one-dimensional semiconductors. However, overcoming lattice mismatch between magnetic nanocrystals and optically active semiconductors remains a major challenge.[107–109]

Remarkably, Yu, Tang, Sargent, and co-workers reported the regioselective magnetization of semiconductor NRs by achieving regioselective nucleation of magnetic nanodomains (Fe_3O_4) at one end of semiconducting NRs (Fig. 9).[70] They reported a strategy for constructing an intermediate buffer layer, which modifies interface energy and promotes selective growth of other incompatible materials in specific regions.[70] To achieve the growth of magnetic Fe_3O_4 on $Zn_xCd_{1-x}S$ with optical activity in the ultraviolet region, Au and Ag_2S, which are highly compatible with both materials, were added as buffer layers to establish connections between them. During the preparation process, Au provided active sites for the growth of Fe_3O_4, while

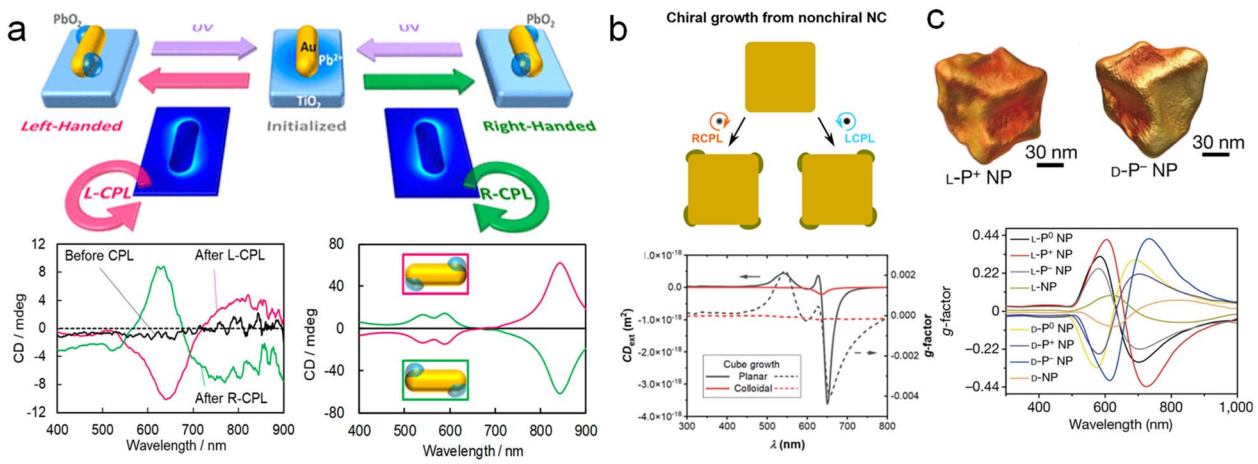

Fig. 8 Circularly polarized light-mediated growth of chiral hybrid nanostructures. (a) Schematics of asymmetric growth of photoinduced PbO_2 on Au NRs and the corresponding experimental and theoretical CD spectra.[105] Reproduced from ref. 105 with permission from American Chemical Society, copyright 2020. (b) Chiral growth of light-manipulated Au nanocubes and corresponding CD and *g*-factor spectra.[65] Reproduced from ref. 65 with permission from American Chemical Society, copyright 2021. (c) Chiral Au NPs are prepared by the interaction of circularly polarized light and chiral molecules.[42] Reproduced from ref. 42 with permission from Springer Nature, copyright 2022.

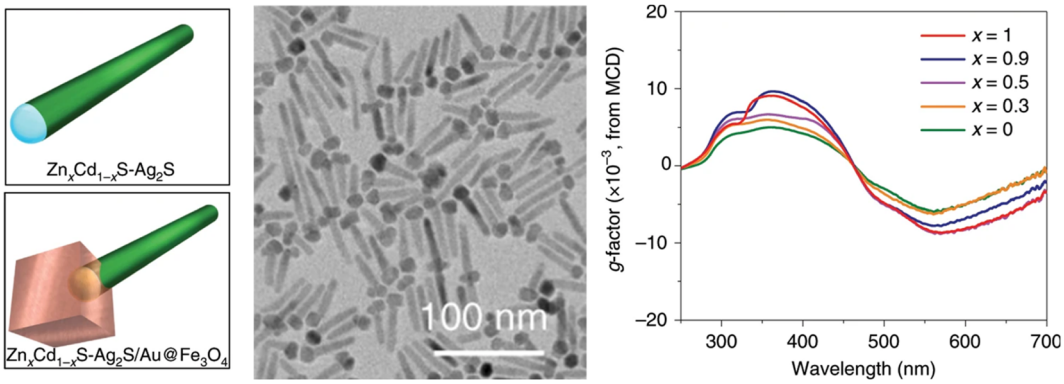

Fig. 9 Multicomponent hybrid materials with magnetically induced chirality. Geometric models, TEM image, and magnetic CD spectra of $Zn_xCd_{1-x}S$-Ag_2S/Au@Fe_3O_4 hybrid materials.[70] Reproduced from ref. 70 with permission from Springer Nature, copyright 2020.

Ag_2S provided growth sites for $Zn_xCd_{1-x}S$, enabling the combination of Fe_3O_4 and $Zn_xCd_{1-x}S$. Unlike traditional chiral materials, although this material lacks distinct chiral structures, distorted lattices, or the pseudo-CD effect, it still exhibits optical chirality in the ultraviolet region (200–400 nm) and shows significant enhancement under a magnetic field. This is attributed to the splitting of the electronic states in the Fe_3O_4 nanodomains under excitation by CPL, resulting in different absorption coefficients. This provides a new strategy for designing chiral multicomponent materials and offers an ideal chiral platform for exploring spin catalysis and spin electronics.

In summary, the selective coupling of the magnetic component with the semiconductor structure can generate chiral optical activity mediated by magnetic fields. Interestingly, how the magnetically induced chirality would interact with the chiral plasmons remains largely unexplored. Future efforts on the construction of plasmon–magnetic hybrid materials could provide interesting results on the chirality–magnetic coupling.

2.7 Chiral assembly

Assembly is a commonly used method for customizing complex structures. It enables the coupling of various components through polymers,[110] proteins,[111] DNA,[112–114] and ligands.[115] The chiral assembly represents a simple and versatile way to combine different components into chiral superstructures that exhibit structural chirality. The combination of elementary units endows life with remarkable diversity, thus understanding and emulating the assembly of biomacromolecules to construct chiral materials holds significant implications. Inducing spatial asymmetry serves as the primary challenge in achieving the transfer of chirality from templates to spatial structures,[7] thereby facilitating the construction of chiral assemblies. At present, chiral assembly has achieved precise manipulation of nanoscale chiral assembly through the design of chiral templates,[27,116,117] thereby serving as highly sensitive biosensing platforms and potential candidates for pharmaceuticals.[118–120]

A typical example is that Liz-Marzán and co-workers demonstrated the utilization of anthraquinone-based oxalamide as elemental units to fabricate chiral fibrous structures, onto which Au NRs assemble *via* non-covalent interactions (Fig. 10a).[110] CD spectroscopy reveals that, apart from the background provided by supramolecular fibers around 400 nm, the structure exhibits pronounced chiroptical activity in the visible and near-IR range. This chiral signal arises from the 3D arrangement of Au NRs and the pivotal role played by Au NRs in chiroptical activity, as supported by control experiments and dipole-coupling numerical simulations. In addition to chiral fibers as templates, biomacromolecules such as DNA and peptides can also serve as templates for chiral assembly.[64,121] Liu and co-workers have overcome the optical limitations associated with asymmetric factors ranging from 10^{-4} to 10^{-2} in traditional chiral inorganic nanostructures, by increasing the asymmetric factor of Au NRs assembly to above 0.1, thereby potentially rivaling liquid crystals (Fig. 10b).[111] By assembling Au NRs through supramolecular interactions with polypeptides, they observed the gradual formation of long-range ordered chiral structures within 10 days, accompanied by an increase in CD optical activity over time. This discovery has successfully been applied to early disease screening. Additional attention should be directed towards these distinguished review articles to delve deeper into the realm of chiral assembly.[116,122]

As previously mentioned, a significant endeavor has been devoted to chiral assembly, providing a solid foundation for constructing multicomponent assemblies. Firstly, the inherent chiral structures of templates can serve as sources of induced chirality. As shown in Fig. 10c,[67] Govorov and co-workers employed tartaric acid as a chiral inducer to fabricate SiO_2 helices with chiral structures. Subsequently, they coupled Au NPs onto the SiO_2 helices, resulting in a remarkably strong cotton effect in the CD signal. After coupling TiO_2 onto Au through electrostatic interactions, the chiral optical activity remained robust. Theoretical simulations provided strong support for the optical chirality of the assembled chiral hybrid structures. Additionally, Kolíbal and co-workers demonstrated the utilization of inorganic WS_2 nanotubes with helical chiral edges as templates for chiral assembly.[123] These templates remained stable at high temperatures and enabled the assembly of chiral metals and semiconductors, thus serving as an ideal platform for constructing chiral plasmon-semiconductor hybrid materials.

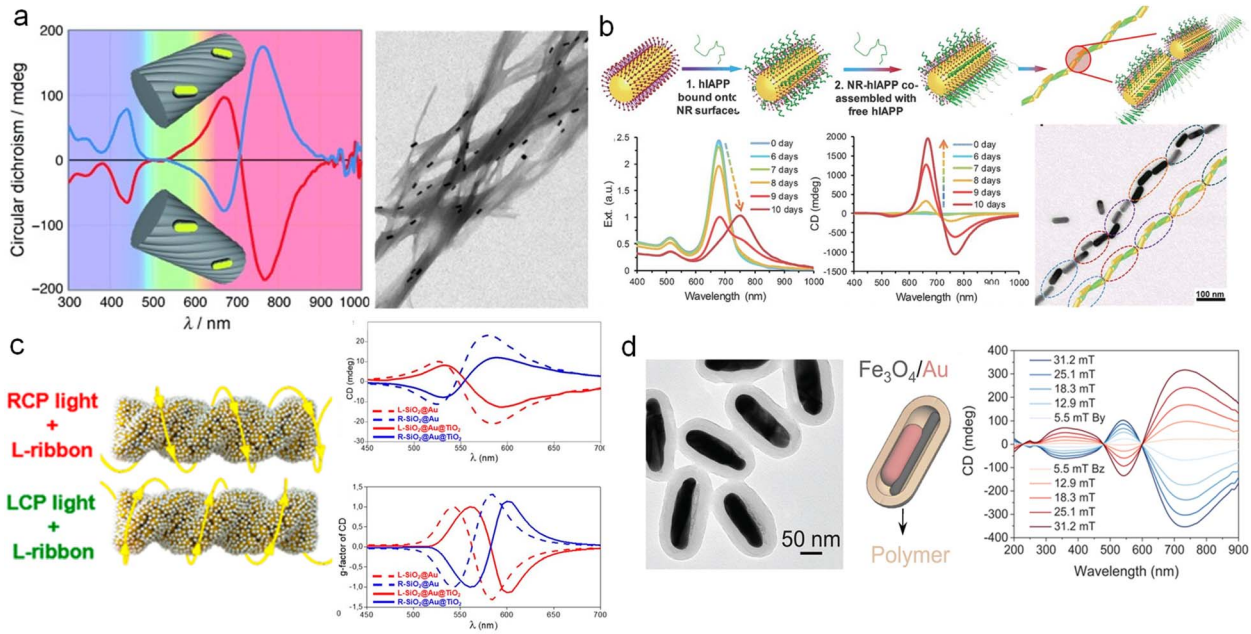

Fig. 10 Preparation of multicomponent chiral plasmonic nanomaterials by chiral assembly. (a) CD spectra and TEM image of Au NR assembly templated by chiral supramolecular fibers.[110] Reproduced from ref. 110 with permission from Wiley VCH, copyright 2011. (b) Schematics, optical properties, and TEM image of long-range ordered assembly of hIAPPs and Au NRs.[111] Reproduced from ref. 111 with permission from AAAS, copyright 2021. (c) Schematic and CD spectra of the SiO_2@Au and SiO_2@Au@TiO_2 nanoribbons.[67] Reproduced from ref. 67 with permission from American Chemical Society, copyright 2022. (d) TEM image of Fe_3O_4/Au hybrid NRs and CD spectra of magnetic-induced chiral superstructures.[124] Reproduced from ref. 124 with permission from AAAS, copyright 2023.

Moreover, the external field also plays a crucial role in inducing chiral assembly.[125] A prominent example is the magnetically controllable chiral superstructures engineered by Yin and co-workers (Fig. 10d).[124] By employing spatially confined growth methods, they synthesized size-controlled Au NRs@Fe_3O_4. The parallel alignment of hybrid NRs facilitated the assembly of chiral superstructures under the influence of a chiral magnetic field, resulting in CD responses that varied with the magnitude of the magnetic field. This approach offers a novel pathway for the chirality transfer modulated by external fields. Moreover, Lee and co-workers synthesized nanostructures Au@Fe_xO_y NWs using a solvothermal process.[126] By inducing a magnetic field, the precise arrangement of high-period photonic structures could be achieved. Manipulating the stacking modes enabled chiral optical control, making it an ideal chiral sensing platform for protein analytes.

As exemplified by the case studies described above, multicomponent chiral plasmonic hybrid nanomaterials with diverse

Table 1 Comparison of methods for the preparation of the multicomponent chiral plasmonic nanomaterials

Method	Advantages	Disadvantages	Ref.
Physical deposition approaches	Ligand-free and can be applied to all diverse components	High cost and reliance on large-scale equipment	85
Galvanic replacement reaction	Ligand-free with precise control over the atomic structure	Limited material variety and difficult to maintain well-defined chiral structure	90
Chiral molecule-mediated growth	Controllable method over both geometry and composition	Difficulties in ruling out the effect of chiral ligands in applications	76
Chiral heterostructure	Tunable geometric control and chiral coupling with diverse structures	Complications in the preparation and limited material variety	99
Circularly polarized light-mediated growth	Ligand-free, simple, and controllable synthesis in chiral structures	Challenging in large-scale preparation and relatively weak in optical chirality	106
Magnetically induced chirality	Unique control over optical chirality using magnetic field	Limited to magnetic materials and related applications	71
Chiral assembly	Strong and tunable optical chirality; can be applied to diverse materials	Challenging in large-scale preparation and reliance on the chiral templates	125

structures have been successfully constructed by using various synthetic techniques. We further summarized the advantages and disadvantages of different preparation methods in a table for readers (Table 1). Notably, the strength and weakness of each method further affect their applications, indicating that we shall consider the application before selecting the synthetic method. It is evident that in recent years, multifunctional chiral hybrid materials have emerged as a rapidly developing research field. This field garners attention not only due to its captivating optical characteristics but also due to the broadened application prospects for multicomponent chiral nanomaterials, offering chiral platforms for emerging technological applications. Thus, in the next section, we focus on the emerging applications of multicomponent chiral plasmonic hybrid nanomaterials.

3. Emerging applications of multicomponent chiral plasmonic hybrid nanomaterials

Compared to single-component chiral plasmonic nanomaterials, multicomponent chiral plasmonic hybrid nanostructures exhibit enhanced physicochemical properties or unexpected properties due to the synergistic couplings among different components. Thus, the introduction of new components holds the potential to bring unexpected changes to chiral plasmonic hybrid nanomaterials, greatly expanding their application prospects. In this section, we review three emerging applications of multicomponent chiral materials, including chirality sensing, enantioselective catalysis, and biomedicine. The primary focus of this review lies in exploring the applications of multicomponent chiral plasmonic hybrid NPs. For a broader overview of the applications of plasmonic chirality, readers are encouraged to further explore excellent review articles in this field.[4,49,127,128]

3.1 Chirality sensing

Chiral plasmonic nanomaterials exhibit not only optical chirality ranging from visible to near-IR spectral regions but also enantioselectivity in response to surface configurations and molecular interactions. Thus, chiral plasmonic NPs can serve as the chirality sensing platform, which provides enantioselective interactions with chiral molecules as well as asymmetric near fields for sensing chiral molecules. Significant efforts have been devoted to utilizing chiral nanomaterials as sensing platforms, successfully applied in enantiomer recognition as well as the detection of disease biomarkers.[28,39,41,51,52]

Multicomponent chiral hybrid nanomaterials have brought more possibilities for the broad application of chirality sensing, particularly with more complex environments. A typical example is that Tang and co-workers developed a chiral hybrid structure for the quantitative detection of chiral enantiomers using SERS (Fig. 11a).[129] By using amino acid-derived chiral surfactants as templates, a layer of chiral mesoporous SiO_2 was grown on Au NRs, exhibiting strong CD optical activity in the visible and near-IR regions. Remarkably, when Cys molecules with the same configuration as the shell template were adsorbed into the SiO_2, a peak appeared at 730 cm^{-1} in the SERS spectra, which was theoretically attributed to the conformational changes of chiral Cys within the mesoporous shell. This method can be used for the quantitative detection of the enantiomeric excess (ee) of Cys isomers. More recently, more chiral hybrid plasmonic materials have been designed and used as excellent substrates for significantly amplifying the molecular vibrational signal, particularly for SERS.[79,130]

Furthermore, the CD signal of chiral plasmonic NPs is also found to be highly sensitive to subtle variations in the external environment or local refractive index.[131,132] Therefore, Niu and co-workers designed Au@Pd chiral NPs for hydrogen sensing (Fig. 11b).[133] By depositing Pd onto chiral Au NPs to construct chiral Au@Pd core–shell structures, the CD signal can be tuned

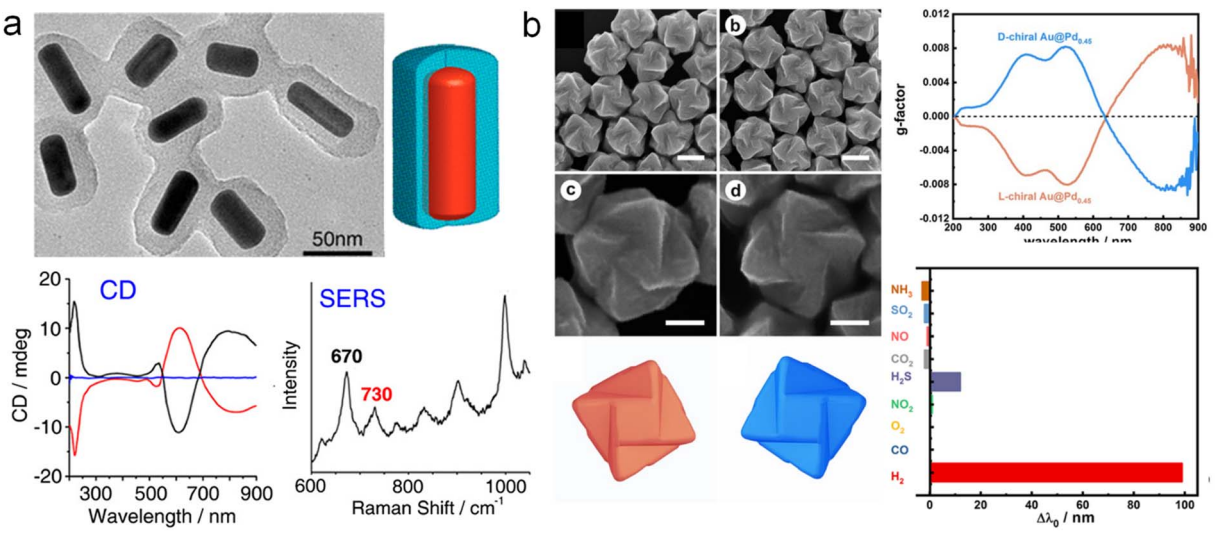

Fig. 11 Chirality sensing using multicomponent chiral plasmon hybrid nanomaterials. (a) Chiral Au NRs@Silica materials for the SERS detection of Cys.[129] Reproduced from ref. 129 with permission from American Chemical Society, copyright 2013. (b) Hydrogen sensing using chiral Au@Pd core–shell NPs.[133] Reproduced from ref. 133 with permission from Wiley VCH, copyright 2023.

by adjusting the amount of deposited Pd. Selecting a Pd content of 0.45 as the sensing platform, a redshift of 206.1 nm was achieved upon exposure to hydrogen. This shift was mainly attributed to the formation of PdH compounds, leading to the LSPR shift in both extinction and CD spectra. Overall, chirality sensing and discrimination are of great importance in diverse fields ranging from biosensing, and pharmaceutics, to asymmetric catalysis. The design of the aforementioned sensing mechanisms based on multicomponent chiral plasmonic hybrid nanomaterials provides new insights for their sensing applications. More efforts shall be focused on both the fundamental understandings and transformative applications of enantioselective sensing using chiral plasmonic NPs.

3.2 Enantioselective catalysis

Chiral plasmonic nanomaterials have been demonstrated as promising catalysts for enantioselective nanocatalysis.[37,38,134,135] However, their application in a wider range of fields is quite limited by the constraints of single-component systems. Especially with regards to current chiral plasmonic materials, due to their advantages in controllable synthesis through wet chemical methods, they are mostly limited to Au, rather than other metals such as Pt, Pd, and Cu, which exhibit higher catalytic activity in many important catalytical reactions. The integration of multiple components into chiral plasmonic nanomaterials has endowed them with potential new functionalities, greatly expanding the catalytic prospects of chiral plasmonic nanomaterials.

The utilization of plasmonic hot carriers for photocatalytic molecular transformation has been widely investigated.[29,136–140] Selectively irradiation of chiral plasmonic materials with CPL could potentially show different capabilities in harnessing plasmonic hot carriers for plasmonic materials with different chiroptical properties. Particularly, Govorov and co-workers demonstrated the construction of chiral TiO_2-Au heterostructures as plasmon-based photocatalysts with polarization-dependent reactivity.[67] It was found that the photocatalytic degradation efficiency is significantly influenced by the CPL irradiation (Fig. 12a). For L-SiO_2@Au@TiO_2, the asymmetric generation efficiency of thermal charges under LH CPL illumination is 2.93 times higher than that under RH CPL illumination, resulting in an increased reaction rate. Further theoretical models demonstrated that the asymmetric photocatalytic properties are the result of polarization-sensitive generation of charge carriers during electromagnetic excitation processes. Similar results on the enantioselective catalytic activities were also observed in the reduction reaction of 4-Nitrophenol (4-NP) catalyzed by chiral Au@Ag NPs.

On the other hand, Xu and co-workers constructed chiral ZnS NPs stabilized by quinidine and induced their assembly to form chiral superstructures, which were further assembled with glutathione-modified Au NPs (Fig. 12b).[141] The structure exhibited CD optical activity ranging from 200 to 550 nm. This binary structure was employed for enantioselective photocatalysis of tyrosine (Tyr). The results showed that L-ZnS-Au superparticles preferentially catalyzed the photooxidation of L-Tyr over D-Tyr, confirming the correlation between the enantioselectivity of photocatalysis and preferential distribution of specific enantiomeric isomers. In summary, despite there being limited work on enantioselective catalysis using multicomponent chiral hybrid plasmonic materials, it shows promise in creating unconventional reaction pathways or mechanisms when applied to traditional catalytic reactions. One main challenge is the relatively weak catalytic activities that have been shown by the multicomponent chiral hybrid plasmonic NPs,

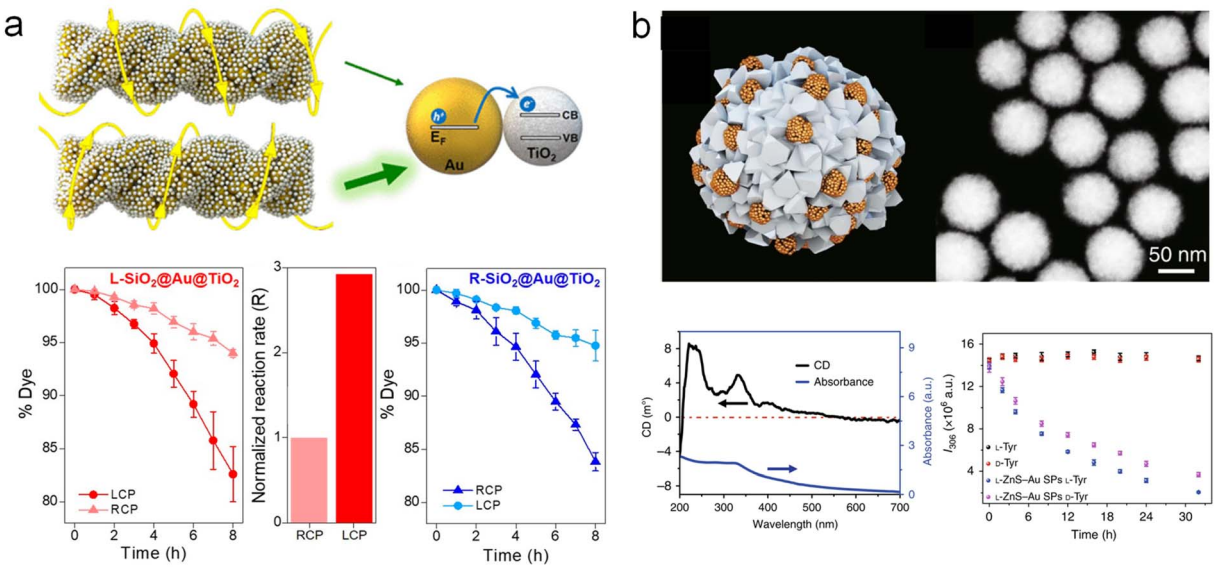

Fig. 12 Enantioselective catalysis using multicomponent chiral plasmonic hybrid materials. (a) Chiral Au/TiO_2 hybrid structures for the realization of the differential chiral photocatalytic degradation of dyes.[67] Reproduced from ref. 67 with permission from American Chemical Society, copyright 2022. (b) Chiral ZnS-Au superstructures and the corresponding enantioselective photocatalytic activities.[141] Reproduced from ref. 141 with permission from Springer Nature, copyright 2019.

which can be further improved by integrating catalytically active components.

3.3 Biomedical applications

Chirality pervades natural life and holds paramount significance within biological systems. Consequently, chiral nanomaterials manifest unique advantages in biological contexts and hold promise as a new generation of therapeutic agents for disease treatment.[142] However, in the realm of biological applications, the size, composition, toxicity, and other attributes of nanomaterials assume critical importance. Therefore, it is of profound significance to undertake the design of chiral inorganic nanomaterials with multifunctional properties, leveraging specific chiral induction of biological effects.

One typical example is that Xu and co-workers designed a chiral AuCuAu NRs hybrid structure and explored their biomedical applications (Fig. 13a).[143] By engendering the growth of Cu on the side facets of Au NRs, AuCu NRs were generated. GRR occurs between Cu and Au ions leading to the formation of chiral AuCuAu NR in the presence of chiral dipeptide, Cys–Phe. Within the wavelength range of 400–1000 nm, the as-prepared chiral hybrid nanostructures exhibit intense and tunable chiroptical activity. The optical chirality originated from the plasmon-coupled CD of chiral molecules in the structure. Subsequent intratumoral injection of chiral AuCuAu NR into mice resulted in their preferential accumulation at the tumor site within a 24 hours timeframe. Following irradiation with CPL, it was observed that L-AuCuAu NR exhibited heightened singlet oxygen production under LH CPL illumination, engendering significant tumor cell eradication. These findings underscore the efficacy of chiral phototherapeutic materials.

Moreover, chiral nanomaterials, as agents capable of circumventing extant acquired resistance mechanisms, have also exhibited exceptional performance in antibacterial domains. Li and co-workers fabricated a chiral Au/MoS_2 hybrid structure, wherein the generation of branched structures induced by Cys conferred conspicuous optical chirality spanning from the visible to the near-IR region (Fig. 13b).[144] Through the synergistic employment of the hybrid structure in conjunction with norfloxacin within a hydrogel, experimental investigations substantiated notable antibacterial activity under infrared photon excitation, with sustained release profiles.

It is also worth highlighting the capability of CPL to exert enantioselective optical forces.[145] In this regard, Kuang and co-workers harnessed chiral branched plasmonic assemblies constructed from Au NPs of varying sizes (30 nm, 20 nm, and 5 nm) for neuron differentiation (Fig. 13c).[146] Experimental and

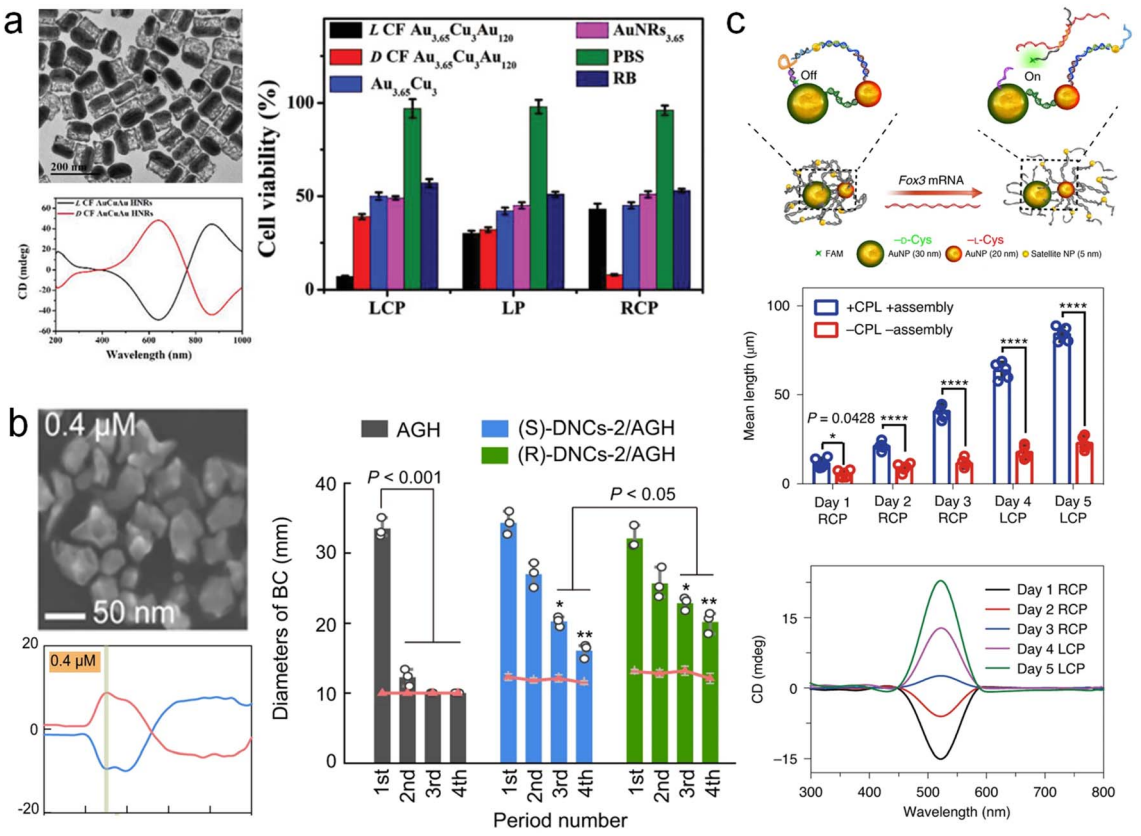

Fig. 13 Biomedical applications of multicomponent chiral plasmonic nanomaterials. (a) Chiral AuCuAu NRs and their applications in selective tumor cell eradication under CPL irradiation.[143] Reproduced from ref. 143 with permission from Wiley VCH, copyright 2020. (b) Chiral MoS_2@Au hybrid materials and their applications in the improvement of the antibacterial activity of levofloxacin gel.[144] Reproduced from ref. 144 with permission from Springer Nature, copyright 2022. (c) Cys-modified chiral Au NPs assemblies and the CPL-induced neural stem cell differentiation.[146] Reproduced from ref. 146 with permission from Springer Nature, copyright 2021.

computational results concur that exposure to CPL engendered augmented neurite outgrowth relative to alternative light conditions, thereby signifying CPL-induced neural stem cell differentiation. This phenomenon derives from the transference of optical forces generated by chiral assemblies to cytoskeletal filaments, thereby fostering heightened differentiation.

Despite the above pioneering efforts, the application of multicomponent chiral plasmonic hybrid nanomaterials across diverse domains remains in its nascent stages. It is urgent to further investigate the rational design of chiral plasmonic nanoparticles possessing desired optical chirality and surface chemical properties. Furthermore, a mechanistic understanding of the functionalities and coupling effects inherent within each constituent, in conjunction with the interactions between light and chiral plasmonic nanomaterials at the interface with substrates, shall furnish robust support for the design and implementation of multicomponent chiral hybrid nanomaterials.

4. Outlook and conclusion

As evidenced by the aforementioned studies, the intriguing properties of multicomponent chiral plasmonic hybrid nanoparticles, coupled with their diverse applications, have engendered enormous interest. However, the practical implementation of these materials still confronts numerous unresolved challenges. Foremost, the prevailing chiral constituents in multicomponent chiral plasmonic hybrid materials primarily focus on Au, owing to its inherent advantages in stability and controllable synthesis. Consequently, there is an imperative demand to vigorously pursue the development of chiral material fabrication methods for other functional materials such as catalytic-active Pt-group metals, semiconductors, and biocompatible polymers, *etc*. Furthermore, the substantial lattice mismatch between different constituents of multicomponent materials remains a formidable impediment in constructing geometrically tunable multicomponent chiral hybrid nanostructures. Hence, it is indubitably critical to embark upon the exploration of novel fabrication approaches for multicomponent chiral hybrid materials, thereby propelling their broader utility. On the other hand, the current synthesis of chiral nanomaterials still relies heavily on laborious experimentation and trial-and-error approaches. For example, the polydispersity in the samples made in the lab is quite arbitrary. Therefore, it is significant to explore how to achieve the prediction of nanomaterials based on existing theories and experimental data.

Moreover, the coupling between chiral plasmons and other functional materials is mechanically complex. Therefore, theoretical understanding along with accurate chiroptical measurements on chiral plasmonic hybrid materials are encouraged to provide more quantitative insights on the mechanistic understanding of chiral coupling. Additionally, the biological toxicity stemming from residual chiral molecules within multicomponent chiral plasmonic hybrid materials, in conjunction with their intricate interplay with target analytes, invariably confounds practical applications and severely limits their potential scope. Thus, one of the future efforts could focus on chemically synthesized chiral hybrid materials in the absence of chiral molecules to avoid complications from surface-absorbed chiral molecules on the enantioselectivity. Finally, to achieve broad applications in the real world, the scale-up and assembly of chiral materials in certain patterns are also very important. The coupling among chiral NPs with controllable gap/orientation could potentially provide unexpected and interesting properties. Therefore, it is urgent to develop a robust method for controlling the patterned assembly of chiral hybrid materials.

In summary, this review comprehensively delineates the controlled fabrication and optical properties of multicomponent plasmonic hybrid nanomaterials, while concurrently outlining their recent advancements in emerging applications. First, we review the typical physical and chemical approaches that have been used to fabricate multicomponent chiral hybrid materials, including the physical deposition approach, chiral molecule-mediated, chiral heterostructure, circularly polarized light-mediated, magnetically induced, and chiral assembly. Second, we discuss present three emerging applications (chirality sensing, enantioselective catalysis, and biomedicine) in which multicomponent chiral plasmonic hybrid materials have attracted enormous interest. Finally, it is envisioned that by taking advantage of the powerful physical and chemical synthesis tools, chiral plasmonic hybrid materials with increasing architectural/compositional diversity and desired optical properties can be achieved, which will substantially promote chirality-based applications in many interdisciplinary areas.

Author contributions

The manuscript was written through the contributions of all authors. All authors have given approval to the final version of the manuscript.

Conflicts of interest

There are no conflicts to declare.

Acknowledgements

This work was supported by the National Natural Science Foundation of China (grant no. 22174104 to Q. Z.). L. S. acknowledges the support of the Hubei Provincial Natural Science Foundation of China (grant no. 2022CFB627) and the Fundamental Research Funds for the Central Universities (grant no. 20422022kf1039). The authors also acknowledge the support of the Large-scale Instrument and Equipment Sharing Foundation of Wuhan University and the Core Facility of Wuhan University.

References

1 U. J. Meierhenrich, *Amino Acids and the Asymmetry of Life*, Springer, Berlin, Heidelberg, 1st edn, 2008.
2 L. Pasteur, *Ann. Chim. Phys.*, 1848, **24**, 442–459.
3 Y. Xia, Y. Zhou and Z. Tang, *Nanoscale*, 2011, **3**, 1374–1382.

4 W. Ma, L. Xu, A. F. de Moura, X. Wu, H. Kuang, C. Xu and N. A. Kotov, *Chem. Rev.*, 2017, **117**, 8041–8093.
5 P. P. Wang, S. J. Yu, A. O. Govorov and M. Ouyang, *Nat. Commun.*, 2017, **8**, 14312.
6 A. Guerrero-Martínez, J. L. Alonso-Gómez, B. Auguié, M. M. Cid and L. M. Liz-Marzán, *Nano Today*, 2011, **6**, 381–400.
7 A. Ben-Moshe, B. M. Maoz, A. O. Govorov and G. Markovich, *Chem. Soc. Rev.*, 2013, **42**, 7028–7041.
8 J. Yeom, U. S. Santos, M. Chekini, M. Cha, A. F. de Moura and N. A. Kotov, *Science*, 2018, **359**, 309–314.
9 Y. Wang, J. Xu, Y. Wang and H. Chen, *Chem. Soc. Rev.*, 2013, **42**, 2930–2962.
10 M. J. Urban, C. Shen, X.-T. Kong, C. Zhu, A. O. Govorov, Q. Wang, M. Hentschel and N. Liu, *Annu. Rev. Phys. Chem.*, 2019, **70**, 275–299.
11 M. Hentschel, M. Schäferling, X. Duan, H. Giessen and N. Liu, *Sci. Adv.*, 2017, **3**, e1602735.
12 X. Wang and Z. Tang, *Small*, 2017, **13**, 1601115.
13 C. Burda, X. Chen, R. Narayanan and M. A. El-Sayed, *Chem. Rev.*, 2005, **105**, 1025–1102.
14 C. E. Talley, J. B. Jackson, C. Oubre, N. K. Grady, C. W. Hollars, S. M. Lane, T. R. Huser, P. Nordlander and N. J. Halas, *Nano Lett.*, 2005, **5**, 1569–1574.
15 M. A. El-Sayed, *Acc. Chem. Res.*, 2001, **34**, 257–264.
16 S. Link and M. A. El-Sayed, *J. Phys. Chem. B*, 1999, **103**, 8410–8426.
17 S. J. Oldenburg, R. D. Averitt, S. L. Westcott and N. J. Halas, *Chem. Phys. Lett.*, 1998, **288**, 243–247.
18 H. Wang, D. W. Brandl, P. Nordlander and N. J. Halas, *Acc. Chem. Res.*, 2007, **40**, 53–62.
19 Y. Xia and N. J. Halas, *MRS Bull.*, 2005, **30**, 338–348.
20 Y. Sun and Y. Xia, *Science*, 2002, **298**, 2176–2179.
21 S. E. Skrabalak, J. Chen, Y. Sun, X. Lu, L. Au, C. M. Cobley and Y. Xia, *Acc. Chem. Res.*, 2008, **41**, 1587–1595.
22 T.-H. Yang, J. Ahn, S. Shi, P. Wang, R. Gao and D. Qin, *Chem. Rev.*, 2021, **121**, 796–833.
23 K. Chen and H. Wang, *Mol. Syst. Des. Eng.*, 2021, **6**, 250–280.
24 S. Eustis and M. A. El-Sayed, *Chem. Soc. Rev.*, 2006, **35**, 209–217.
25 L. M. Kneer, E.-M. Roller, L. V. Besteiro, R. Schreiber, A. O. Govorov and T. Liedl, *ACS Nano*, 2018, **12**, 9110–9115.
26 J. M. Slocik, A. O. Govorov and R. R. Naik, *Nano Lett.*, 2011, **11**, 701–705.
27 Q. Zhang, T. Hernandez, K. W. Smith, S. A. Hosseini Jebeli, A. X. Dai, L. Warning, R. Baiyasi, L. A. McCarthy, H. Guo, D.-H. Chen, J. A. Dionne, C. F. Landes and S. Link, *Science*, 2019, **365**, 1475–1478.
28 L. A. Warning, A. R. Miandashti, L. A. McCarthy, Q. Zhang, C. F. Landes and S. Link, *ACS Nano*, 2021, **15**, 15538–15566.
29 D. F. Swearer, H. Zhao, L. Zhou, C. Zhang, H. Robatjazi, J. M. P. Martirez, C. M. Krauter, S. Yazdi, M. J. McClain, E. Ringe, E. A. Carter, P. Nordlander and N. J. Halas, *Proc. Natl. Acad. Sci. U. S. A.*, 2016, **113**, 8916–8920.
30 A. B. Zrimsek, N. Chiang, M. Mattei, S. Zaleski, M. O. McAnally, C. T. Chapman, A.-I. Henry, G. C. Schatz and R. P. Van Duyne, *Chem. Rev.*, 2017, **117**, 7583–7613.
31 H. Xu, E. J. Bjerneld, M. Käll and L. Börjesson, *Phys. Rev. Lett.*, 1999, **83**, 4357–4360.
32 J. Zheng, X. Cheng, H. Zhang, X. Bai, R. Ai, L. Shao and J. Wang, *Chem. Rev.*, 2021, **121**, 13342–13453.
33 N. J. Halas, S. Lal, W. S. Chang, S. Link and P. Nordlander, *Chem. Rev.*, 2011, **111**, 3913–3961.
34 Z. Fan and A. O. Govorov, *Nano Lett.*, 2012, **12**, 3283–3289.
35 A. O. Govorov, Z. Fan, P. Hernandez, J. M. Slocik and R. R. Naik, *Nano Lett.*, 2010, **10**, 1374–1382.
36 J. K. Gansel, M. Thiel, M. S. Rill, M. Decker, K. Bade, V. Saile, G. von Freymann, S. Linden and M. Wegener, *Science*, 2009, **325**, 1513–1515.
37 L. Ruiyi, W. Xiaobo, P. Yuanfeng, X. Pengwu, Z. Haiyan, L. Zaijun and S. Xiulan, *Catal. Sci. Technol.*, 2022, **12**, 2097–2105.
38 Y. Fang, X. Liu, J. Ai, G. Zhao, L. Chen, S. Che and L. Han, *Chem. Mater.*, 2023, **35**, 2402–2407.
39 R. M. Kim, J.-H. Huh, S. Yoo, T. G. Kim, C. Kim, H. Kim, J. H. Han, N. H. Cho, Y.-C. Lim, S. W. Im, E. Im, J. R. Jeong, M. H. Lee, T.-Y. Yoon, H.-Y. Lee, Q. H. Park, S. Lee and K. T. Nam, *Nature*, 2022, **612**, 470–476.
40 S. X. Leong, C. S. L. Koh, H. Y. F. Sim, Y. H. Lee, X. Han, G. C. Phan-Quang and X. Y. Ling, *ACS Nano*, 2021, **15**, 1817–1825.
41 Z. Liu, J. Ai, P. Kumar, E. You, X. Zhou, X. Liu, Z. Tian, P. Bour, Y. Duan, L. Han, N. A. Kotov, S. Ding and S. Che, *Angew. Chem., Int. Ed.*, 2020, **59**, 15226–15231.
42 L. Xu, X. Wang, W. Wang, M. Sun, W. J. Choi, J.-Y. Kim, C. Hao, S. Li, A. Qu, M. Lu, X. Wu, F. M. Colombari, W. R. Gomes, A. L. Blanco, A. F. de Moura, X. Guo, H. Kuang, N. A. Kotov and C. Xu, *Nature*, 2022, **601**, 366–373.
43 N.-N. Zhang, H.-R. Sun, S. Liu, Y.-C. Xing, J. Lu, F. Peng, C.-L. Han, Z. Wei, T. Sun, B. Yang and K. Liu, *CCS Chem.*, 2022, **4**, 660–670.
44 A. Kuzyk, R. Schreiber, Z. Fan, G. Pardatscher, E. M. Roller, A. Hogele, F. C. Simmel, A. O. Govorov and T. Liedl, *Nature*, 2012, **483**, 311–314.
45 X. Lan, Z. Chen, G. Dai, X. Lu, W. Ni and Q. Wang, *J. Am. Chem. Soc.*, 2013, **135**, 11441–11444.
46 X. Shen, A. Asenjo-Garcia, Q. Liu, Q. Jiang, F. J. García de Abajo, N. Liu and B. Ding, *Nano Lett.*, 2013, **13**, 2128–2133.
47 M. J. Urban, P. K. Dutta, P. Wang, X. Duan, X. Shen, B. Ding, Y. Ke and N. Liu, *J. Am. Chem. Soc.*, 2016, **138**, 5495–5498.
48 N. H. Cho, A. Guerrero-Martínez, J. Ma, S. Bals, N. A. Kotov, L. M. Liz-Marzán and K. T. Nam, *Nat. Rev. Bioeng.*, 2023, **1**, 88–106.
49 L. Sun, Y. Tao, G. Yang, C. Liu, X. Sun and Q. Zhang, *Adv. Mater.*, 2023, e2306297, DOI: **10.1002/adma.202306297**.
50 H. E. Lee, H. Y. Ahn, J. Mun, Y. Y. Lee, M. Kim, N. H. Cho, K. Chang, W. S. Kim, J. Rho and K. T. Nam, *Nature*, 2018, **556**, 360–365.
51 R. Tullius, A. S. Karimullah, M. Rodier, B. Fitzpatrick, N. Gadegaard, L. D. Barron, V. M. Rotello, G. Cooke, A. Lapthorn and M. Kadodwala, *J. Am. Chem. Soc.*, 2015, **137**, 8380–8383.

52 E. Hendry, T. Carpy, J. Johnston, M. Popland, R. V. Mikhaylovskiy, A. J. Lapthorn, S. M. Kelly, L. D. Barron, N. Gadegaard and M. Kadodwala, *Nat. Nanotechnol.*, 2010, **5**, 783–787.
53 K. W. Smith, L. A. McCarthy, A. Alabastri, L. Bursi, W.-S. Chang, P. Nordlander and S. Link, *ACS Nano*, 2018, **12**, 11657–11663.
54 L. A. McCarthy, S. A. Hosseini Jebeli and S. Link, *J. Phys. Chem. C*, 2021, **125**, 4092–4101.
55 L. Xiao, T. An, L. Wang, X. Xu and H. Sun, *Nano Today*, 2020, **30**, 100824.
56 Z. Cao, H. Gao, M. Qiu, W. Jin, S. Deng, K. Y. Wong and D. Lei, *Adv. Mater.*, 2020, **32**, e1905758.
57 Y. Duan and S. Che, *Adv. Mater.*, 2022, e2205088, DOI: 10.1002/adma.202205088.
58 W. Wu and M. Pauly, *Adv. Mater.*, 2022, **3**, 186–215.
59 H.-Y. Ahn, S. Yoo, N. H. Cho, R. M. Kim, H. Kim, J.-H. Huh, S. Lee and K. T. Nam, *Acc. Chem. Res.*, 2019, **52**, 2768–2783.
60 H.-E. Lee, R. M. Kim, H.-Y. Ahn, Y. Y. Lee, G. H. Byun, S. W. Im, J. Mun, J. Rho and K. T. Nam, *Nat. Commun.*, 2020, **11**, 263.
61 Y. Tao, L. Sun, C. Liu, G. Yang, X. Sun and Q. Zhang, *Small*, 2023, **19**, 2301218.
62 X. Sun, J. Yang, L. Sun, G. Yang, C. Liu, Y. Tao, Q. Cheng, C. Wang, H. Xu and Q. Zhang, *ACS Nano*, 2022, **16**, 19174–19186.
63 J. Karst, N. H. Cho, H. Kim, H.-E. Lee, K. T. Nam, H. Giessen and M. Hentschel, *ACS Nano*, 2019, **13**, 8659–8668.
64 X. Lan, X. Zhou, L. A. McCarthy, A. O. Govorov, Y. Liu and S. Link, *J. Am. Chem. Soc.*, 2019, **141**, 19336–19341.
65 L. V. Besteiro, A. Movsesyan, O. Avalos-Ovando, S. Lee, E. Cortes, M. A. Correa-Duarte, Z. M. Wang and A. O. Govorov, *Nano Lett.*, 2021, **21**, 10315–10324.
66 B. Auguié, J. L. Alonso-Gómez, A. Guerrero-Martínez and L. M. Liz-Marzán, *J. Phys. Chem. Lett.*, 2011, **2**, 846–851.
67 Y. Negrin-Montecelo, A. Movsesyan, J. Gao, S. Burger, Z. M. Wang, S. Nlate, E. Pouget, R. Oda, M. Comesana-Hermo, A. O. Govorov and M. A. Correa-Duarte, *J. Am. Chem. Soc.*, 2022, **144**, 1663–1671.
68 G. Zheng, S. Jiao, W. Zhang, S. Wang, Q. Zhang, L. Gu, W. Ye, J. Li, X. Ren, Z. Zhang and K.-Y. Wong, *Nano Res.*, 2022, **15**, 6574–6581.
69 H. Liu, A. E. Vladar, P. P. Wang and M. Ouyang, *J. Am. Chem. Soc.*, 2023, **145**, 7495–7503.
70 T. T. Zhuang, Y. Li, X. Gao, M. Wei, F. P. Garcia de Arquer, P. Todorovic, J. Tian, G. Li, C. Zhang, X. Li, L. Dong, Y. Song, Y. Lu, X. Yang, L. Zhang, F. Fan, S. O. Kelley, S. H. Yu, Z. Tang and E. H. Sargent, *Nat. Nanotechnol.*, 2020, **15**, 192–197.
71 F. Wu, Y. Tian, X. Luan, X. Lv, F. Li, G. Xu and W. Niu, *Nano Lett.*, 2022, **22**, 2915–2922.
72 B. Ni, M. Mychinko, S. Gomez-Grana, J. Morales-Vidal, M. Obelleiro-Liz, W. Heyvaert, D. Vila-Liarte, X. Zhuo, W. Albrecht, G. Zheng, G. Gonzalez-Rubio, J. M. Taboada, F. Obelleiro, N. Lopez, J. Perez-Juste, I. Pastoriza-Santos, H. Colfen, S. Bals and L. M. Liz-Marzan, *Adv. Mater.*, 2023, **35**, e2208299.
73 W. Jiang, Z.-b. Qu, P. Kumar, D. Vecchio, Y. Wang, Y. Ma, J. H. Bahng, K. Bernardino, W. R. Gomes, F. M. Colombari, A. Lozada-Blanco, M. Veksler, E. Marino, A. Simon, C. Murray, S. R. Muniz, A. F. de Moura and N. A. Kotov, *Science*, 2020, **368**, 642–648.
74 S. W. Im, H.-Y. Ahn, R. M. Kim, N. H. Cho, H. Kim, Y.-C. Lim, H.-E. Lee and K. T. Nam, *Adv. Mater.*, 2020, **32**, 1905758.
75 J. Chen, X. Gao, Q. Zheng, J. Liu, D. Meng, H. Li, R. Cai, H. Fan, Y. Ji and X. Wu, *ACS Nano*, 2021, **15**, 15114–15122.
76 X. Zhuo, D. Vila-Liarte, S. Wang, D. Jimenez de Aberasturi and L. M. Liz-Marzán, *Chem. Mater.*, 2023, **35**, 5689–5698.
77 G. González-Rubio, J. Mosquera, V. Kumar, A. Pedrazo-Tardajos, P. Llombart, D. M. Solís, I. Lobato, E. G. Noya, A. Guerrero-Martínez, J. M. Taboada, F. Obelleiro, L. G. MacDowell, S. Bals and L. M. Liz-Marzán, *Science*, 2020, **368**, 1472–1477.
78 X. Zhuo, M. Mychinko, W. Heyvaert, D. Larios, M. Obelleiro-Liz, J. M. Taboada, S. Bals and L. M. Liz-Marzán, *ACS Nano*, 2022, **16**, 19281–19292.
79 P. Yang, Q. Deng, Y. Duan, Z. Liu, Y. Fang, L. Han and S. Che, *Adv. Mater. Interfaces*, 2022, **9**, 2200369.
80 L. Tan, Z. Wen, Z. Geng, Y. Jin, H. Wu and P.-p. Wang, *Chem. Res. Chin. Univ.*, 2023, **39**, 642–646.
81 M. Esposito, V. Tasco, M. Cuscunà, F. Todisco, A. Benedetti, I. Tarantini, M. D. Giorgi, D. Sanvitto and A. Passaseo, *ACS Photonics*, 2015, **2**, 105–114.
82 C.-Y. Ji, S. Chen, Y. Han, X. Liu, J. Liu, J. Li and Y. Yao, *Nano Lett.*, 2021, **21**, 6828–6834.
83 Y. Hou, H. M. Leung, C. T. Chan, J. Du, H. L.-W. Chan and D. Y. Lei, *Adv. Funct. Mater.*, 2016, **26**, 7807–7816.
84 A. G. Mark, J. G. Gibbs, T. C. Lee and P. Fischer, *Nat. Mater.*, 2013, **12**, 802–807.
85 J. Liu, L. Yang and Z. Huang, *Small*, 2016, **12**, 5902–5909.
86 J. Liu, L. Yang, H. Zhang, J. Wang and Z. Huang, *Small*, 2017, **13**, 1701112.
87 L. Yang, P. Nandi, Y. Ma, J. Liu, U. Mirsaidov and Z. Huang, *Small*, 2020, **16**, e1906048.
88 J. Ahn, D. Wang, Y. Ding, J. Zhang and D. Qin, *ACS Nano*, 2018, **12**, 298–307.
89 J. Liu, Z. Ni, P. Nandi, U. Mirsaidov and Z. Huang, *Nano Lett.*, 2019, **19**, 7427–7433.
90 Z. Ni, Y. Zhu, J. Liu, L. Yang, P. Sun, M. Gu and Z. Huang, *Adv. Sci.*, 2020, **7**, 2001321.
91 A. Wolf, T. Kodanek and D. Dorfs, *Nanoscale*, 2015, **7**, 19519–19527.
92 S. Lambright, E. Butaeva, N. Razgoniaeva, T. Hopkins, B. Smith, D. Perera, J. Corbin, E. Khon, R. Thomas, P. Moroz, A. Mereshchenko, A. Tarnovsky and M. Zamkov, *ACS Nano*, 2014, **8**, 352–361.
93 M. R. Buck, J. F. Bondi and R. E. Schaak, *Nat. Chem.*, 2012, **4**, 37–44.
94 A. Figuerola, I. R. Franchini, A. Fiore, R. Mastria, A. Falqui, G. Bertoni, S. Bals, G. Van Tendeloo, S. Kudera, R. Cingolani and L. Manna, *Adv. Mater.*, 2009, **21**, 550–554.

95 J. W. Kim, N. H. Cho, R. M. Kim, J. H. Han, S. Choi, S. D. Namgung, H. Kim and K. T. Nam, *Nano Lett.*, 2022, **22**, 8181–8188.
96 G. Zheng, Z. Bao, J. Perez-Juste, R. Du, W. Liu, J. Dai, W. Zhang, L. Y. S. Lee and K. Y. Wong, *Angew. Chem., Int. Ed.*, 2018, **57**, 16452–16457.
97 H. Kim, E. Im, R. M. Kim, N. H. Cho, J. H. Han, H.-Y. Ahn, J.-H. Huh, S. Yoo, S. Lee and K. T. Nam, *Adv. Opt. Mater.*, 2023, **11**, 2300205.
98 G. Yang, L. Sun, Y. Tao, Q. Cheng, X. Sun, C. Liu and Q. Zhang, *Sci. China: Chem.*, 2023, **66**, 3280–3289.
99 S. Linic, P. Christopher and D. B. Ingram, *Nat. Mater.*, 2011, **10**, 911–921.
100 M. J. Kale, T. Avanesian and P. Christopher, *ACS Catal.*, 2013, **4**, 116–128.
101 O. Ávalos-Ovando, E. Y. Santiago, A. Movsesyan, X.-T. Kong, P. Yu, L. V. Besteiro, L. K. Khorashad, H. Okamoto, J. M. Slocik, M. A. Correa-Duarte, M. Comesaña-Hermo, T. Liedl, Z. Wang, G. Markovich, S. Burger and A. O. Govorov, *ACS Photonics*, 2022, **9**, 2219–2236.
102 H. Wang, Y. Liu, J. Yu, Y. Luo, L. Wang, T. Yang, B. Raktani and H. Lee, *ACS Appl. Mater. Interfaces*, 2022, **14**, 3559–3567.
103 J. Y. Kim, J. Yeom, G. Zhao, H. Calcaterra, J. Munn, P. Zhang and N. Kotov, *J. Am. Chem. Soc.*, 2019, **141**, 11739–11744.
104 K. Saito and T. Tatsuma, *Nano Lett.*, 2018, **18**, 3209–3212.
105 K. Morisawa, T. Ishida and T. Tatsuma, *ACS Nano*, 2020, **14**, 3603–3609.
106 G. Singh, H. Chan, A. Baskin, E. Gelman, N. Repnin, P. Král and R. Klajn, *Science*, 2014, **345**, 1149–1153.
107 J. Lee, J. Yang, S. G. Kwon and T. Hyeon, *Nat. Rev. Mater.*, 2016, **1**, 16034.
108 C. Tan, J. Chen, X.-J. Wu and H. Zhang, *Nat. Rev. Mater.*, 2018, **3**, 17089.
109 J. Liu and J. Zhang, *Chem. Rev.*, 2020, **120**, 2123–2170.
110 A. Guerrero-Martinez, B. Auguie, J. L. Alonso-Gomez, Z. Dzolic, S. Gomez-Grana, M. Zinic, M. M. Cid and L. M. Liz-Marzán, *Angew. Chem., Int. Ed.*, 2011, **50**, 5499–5503.
111 J. Lu, Y. Xue, K. Bernardino, N.-N. Zhang, W. R. Gomes, N. S. Ramesar, S. Liu, Z. Hu, T. Sun, A. F. de Moura, N. A. Kotov and K. Liu, *Science*, 2021, **371**, 1368–1374.
112 W. Yan, L. Xu, C. Xu, W. Ma, H. Kuang, L. Wang and N. A. Kotov, *J. Am. Chem. Soc.*, 2012, **134**, 15114–15121.
113 L. Weller, V. V. Thacker, L. O. Herrmann, E. A. Hemmig, A. Lombardi, U. F. Keyser and J. J. Baumberg, *ACS Photonics*, 2016, **3**, 1589–1595.
114 H. Lee, J.-H. Lee, S. M. Jin, Y. D. Suh and J.-M. Nam, *Nano Lett.*, 2013, **13**, 6113–6121.
115 T. A. Gschneidtner, Y. A. D. Fernandez, S. Syrenova, F. Westerlund, C. Langhammer and K. Moth-Poulsen, *Langmuir*, 2014, **30**, 3041–3050.
116 C. Zhou, X. Duan and N. Liu, *Acc. Chem. Res.*, 2017, **50**, 2906–2914.
117 K. J. Jeong, D. K. Lee, V. T. Tran, C. Wang, J. Lv, J. Park, Z. Tang and J. Lee, *ACS Nano*, 2020, **14**, 7152–7160.
118 X. Wu, L. Xu, W. Ma, L. Liu, H. Kuang, N. A. Kotov and C. Xu, *Adv. Mater.*, 2016, **28**, 5907–5915.
119 W. Ma, H. Kuang, L. Xu, L. Ding, C. Xu, L. Wang and N. A. Kotov, *Nat. Commun.*, 2013, **4**, 2689.
120 J. Kumar, H. Erana, E. Lopez-Martinez, N. Claes, V. F. Martin, D. M. Solis, S. Bals, A. L. Cortajarena, J. Castilla and L. M. Liz-Marzan, *Proc. Natl. Acad. Sci. U. S. A.*, 2018, **115**, 3225–3230.
121 L. A. Warning, A. R. Miandashti, A. Misiura, C. F. Landes and S. Link, *J. Phys. Chem. C*, 2022, **126**, 2656–2668.
122 J. Lv, X. Gao, B. Han, Y. Zhu, K. Hou and Z. Tang, *Nat. Rev. Chem.*, 2022, **6**, 125–145.
123 L. Kachtik, D. Citterberg, K. Bukvisova, L. Kejik, F. Ligmajer, M. Kovarik, T. Musalek, M. Krishnappa, T. Sikola and M. Kolíbal, *Nano Lett.*, 2023, **23**, 6010–6017.
124 Z. Li, Q. Fan, Z. Ye, C. Wu, Z. Wang and Y. Yin, *Science*, 2023, **380**, 1384–1390.
125 W. Zhao, W. Zhang, R. Y. Wang, Y. Ji, X. Wu and X. Zhang, *Adv. Funct. Mater.*, 2019, **29**, 1900587.
126 H. Q. Nguyen, D. Hwang, S. Park, M. T. Nguyen, S. S. Kang, V. T. Tran and J. Lee, *ACS Nano*, 2022, **16**, 5795–5806.
127 S. Wang, X. Liu, S. Mourdikoudis, J. Chen, W. Fu, Z. Sofer, Y. Zhang, S. Zhang and G. Zheng, *ACS Nano*, 2022, **16**, 19789–19809.
128 G. Zheng, J. He, V. Kumar, S. Wang, I. Pastoriza-Santos, J. Perez-Juste, L. M. Liz-Marzan and K. Y. Wong, *Chem. Soc. Rev.*, 2021, **50**, 3738–3754.
129 W. Liu, Z. Zhu, K. Deng, Z. Li, Y. Zhou, H. Qiu, Y. Gao, S. Che and Z. Tang, *J. Am. Chem. Soc.*, 2013, **135**, 9659–9664.
130 G. Wang, C. Hao, W. Ma, A. Qu, C. Chen, J. Xu, C. Xu, H. Kuang and L. Xu, *Adv. Mater.*, 2021, **33**, 2102337.
131 M. Matuschek, D. P. Singh, H. H. Jeong, M. Nesterov, T. Weiss, P. Fischer, F. Neubrech and N. Liu, *Small*, 2018, **14**, 1702990.
132 H. Lin, H. Mitomo, Y. Yonamine, Z. Guo and K. Ijiro, *Chem. Mater.*, 2022, **34**, 4062–4072.
133 X. Lv, F. Wu, Y. Tian, P. Zuo, F. Li, G. Xu and W. Niu, *Adv. Mater.*, 2023, 2305429.
134 Y. Zhou, H. Sun, H. Xu, S. Matysiak, J. Ren and X. Qu, *Angew. Chem., Int. Ed.*, 2018, **57**, 16791–16795.
135 K. Dong, C. Xu, J. Ren and X. Qu, *Angew. Chem., Int. Ed.*, 2022, **61**, e202208757.
136 S. Mukherjee, F. Libisch, N. Large, O. Neumann, L. V. Brown, J. Cheng, J. B. Lassiter, E. A. Carter, P. Nordlander and N. J. Halas, *Nano Lett.*, 2013, **13**, 240–247.
137 L. Zhou, D. F. Swearer, C. Zhang, H. Robatjazi, H. Zhao, L. Henderson, L. Dong, P. Christopher, E. A. Carter, P. Nordlander and N. J. Halas, *Science*, 2018, **362**, 69–72.
138 X. Zhang, X. Li, M. E. Reish, D. Zhang, N. Q. Su, Y. Gutiérrez, F. Moreno, W. Yang, H. O. Everitt and J. Liu, *Nano Lett.*, 2018, **18**, 1714–1723.
139 Q. Zhang, K. Chen and H. Wang, *J. Phys. Chem. C*, 2021, **125**, 20958–20971.
140 Q. Zhang, Y. Zhou, X. Fu, E. Villarreal, L. Sun, S. Zou and H. Wang, *J. Phys. Chem. C*, 2019, **123**, 26695–26704.

141 S. Li, J. Liu, N. S. Ramesar, H. Heinz, L. Xu, C. Xu and N. A. Kotov, *Nat. Commun.*, 2019, **10**, 4826.
142 B. Ma and A. Bianco, *Nat. Rev. Mater.*, 2023, **8**, 403–413.
143 J. Wang, X. Wu, W. Ma and C. Xu, *Adv. Funct. Mater.*, 2020, **30**, 2000670.
144 B. L. Li, J. J. Luo, H. L. Zou, Q. M. Zhang, L. B. Zhao, H. Qian, H. Q. Luo, D. T. Leong and N. B. Li, *Nat. Commun.*, 2022, **13**, 7289.
145 B. Shi, J. Zhao, Z. Xu, C. Chen, L. Xu, C. Xu, M. Sun and H. Kuang, *Adv. Sci.*, 2022, **9**, e2202475.
146 A. Qu, M. Sun, J. Y. Kim, L. Xu, C. Hao, W. Ma, X. Wu, X. Liu, H. Kuang, N. A. Kotov and C. Xu, *Nat. Biomed. Eng.*, 2021, **5**, 103–113.